A&A 378, 370–393 (2001)
DOI: 10.1051/0004-6361:20011241

Astronomy & Astrophysics

HI observations of loose galaxy groups

I. Data and global properties

W. van Driel[1,2], P. Marcum[3], J. S. Gallagher III[4], E. Wilcots[4], C. Guidoux[5], and D. Monnier Ragaigne[1]

[1] DAEC, UMR CNRS 8631, Observatoire de Paris, Section de Meudon, 5 place Jules Janssen, 92195 Meudon Cedex, France
e-mail: wim.vandriel@obspm.fr; delphine.ragaigne@obspm.fr
[2] Unité Scientifique Nançay, USR CNRS B704, Observatoire de Paris, 18330 Nançay, France
[3] Department of Physics and Astronomy, Texas Christian University, Box 298840, Fort Worth, TX 76129, USA
e-mail: p.marcum@tcu.edu
[4] Astronomy Department, University of Madison-Wisconsin, 475 N. Charter St., Madison WI 53706-1582, USA
e-mail: jsg@astro.wisc.edu; ewilcots@astro.wisc.edu
[5] Faculté des Sciences et des Techniques, Université de Tours, Avenue Monge, 37000 Tours, France

Received 24 July 2001 / Accepted 4 September 2001

Abstract. At Nançay, 21-cm H I line observations were made of 15 spiral-dominated loose groups of galaxies, divided into two samples: an "interacting" sample containing at least one pair of interacting galaxies, and a "control" sample having no optical evidence of interactions or morphological disturbances among the group members. The interacting sample consists of 62 galaxies representing 9 different groups, and the control sample contains 40 galaxies representing 6 groups. Of the 91 galaxy and galaxy pairs observed, 74 were detected, while upper limits were placed on the remaining 17 objects. These homogeneous H I data, which will be used in future analyses, provide comparative information on the H I content of groups and serve as a probe of the vicinity of the target spirals for H I clouds or very low surface brightness gas-rich galaxies.

Key words. galaxies: distances and redshifts – galaxies: general – galaxies: interactions – galaxies: ISM – radio lines: galaxies

1. Introduction

Sufficient evidence now exists to support the idea that at least some groups of galaxies are gravitationally bound entities, and are not merely chance projections or transient clumpiness (Hernquist et al. 1995; Ostriker et al. 1995) in the background of galaxies (Mamon 1986; Rose 1977, 1979). The majority of this evidence comes from X-ray observations which have revealed that some groups are enveloped in a diffuse, hot intra-group gas (Bahcall et al. 1984; Biermann & Kronberg 1984; Mahdavi et al. 1997; Fukazawa et al. 1996; Mulchaey et al. 1996; Davis et al. 1999), analogous to the hot medium seen within dense clusters. The higher the elliptical population within a group, the higher the probability that the group will have an intragroup medium that is detectable by ROSAT (Mulchaey et al. 1996; Mahdavi et al. 1997).

However, the non-detection of a hot, intragroup medium within spiral-rich galaxy groups does not preclude those groups from being real physical systems. The dynamical evolution of a bound group will influence the temperature of the intragroup medium (Mulchaey & Zabludoff 1998), analogous to correlations such as that seen between L_x, T_x and velocity dispersion in galaxy clusters (Xue & Wu 2000). Some studies (Marcum 1994; Hickson et al. 1988; Nolthenius 1993) show that, on average, spiral-rich groups have lower velocity dispersions as compared to elliptical-dominated systems. This reduction in the thermal energy being deposited into the intragroup medium of spiral-rich groups predicts that the extant intergalactic gas in these systems would most likely exist mainly in the form of neutral hydrogen. Indeed, some groups have been found to be rich in neutral hydrogen which is tied up in either low surface brightness dwarfs (Gallagher et al. 1995) or H I clouds (e.g., Schneider et al. 1986b; Hoffman et al. 1992).

Send offprint requests to: W. van Driel,
e-mail: wim.vandriel@obspm.fr

Table 1. Group properties.

GH No. (1)	NGal (2)	RA (2000.0) (3)	Dec.	$<V_{\rm vir}>$ ($\rm km\,s^{-1}$) (4)	σ_V ($\rm km\,s^{-1}$) (5)	d (Mpc) (6)	$B_{\rm T}$ (mag) (7)
Interacting group sample							
45	4	09 16.8	41 17	1833	150	24.4	12.4
58	10	10 19.5	20 46	1319	217	17.6	10.1
67	8	10 51.4	33 35	1814	174	24.2	10.7
86	3	11 37.6	32 09	2806	41	37.4	12.4
92	11	11 54.9	25 29	4361	518	58.1	11.8
126	6	13 56.1	37 40	3532	357	47.1	11.3
141	13	14 23.9	36 01	3683	461	49.1	10.6
153	3	15 26.3	41 17	2790	45	37.2	12.7
156	4	15 34.8	15 30	2040	93	27.2	11.6
Control group sample							
49	3	09 50.5	43 44	4889	65	65.2	12.3
57	4	10 13.6	03 21	1248	60	16.6	10.6
89	7	11 42.5	09 46	6118	180	81.6	11.8
118	3	13 25.4	36 14	5537	254	73.8	12.7
123	17	13 51.3	40 53	2600	158	34.6	9.8
155	6	15 34.0	43 16	5933	149	79.1	12.1

Note: mean group velocities $V_{\rm vir}$ were corrected for Virgocentric infall, and $H_0 = 75\ \rm km\,s^{-1}\ Mpc^{-1}$ was assumed.

The dynamical evolution of a loose group is undoubtedly actuated by multiple minor mergers between these gas-rich satellites and larger group members (Haynes et al. 2000), as well as the more dramatic interactions between the large mass galaxies. While the ramifications of such encounters can be found across the spectrum (such as Hα, B and thermal infrared luminosity enhancements resulting from the ensuing star formation activity, and optical morphological signatures such as tidal tails and bridges), there is evidence that the disruptions in the gaseous disk is long-lived. For example, the presence of X-shaped structures seen in some peculiar S0 galaxies (Mihos et al. 1995), and the counter-rotating disks seen in some early-type spirals (Corsini et al. 1998; Jore et al. 1996) in otherwise optically normal-looking galaxies is interpreted as the aftermath of minor mergers. The outer regions of gas disks are vulnerable to warps and other distortions created by a close encounter with a passing galaxy, and are not likely to rebound quickly once disturbed. The denser regions of a galaxy cluster environment, where galaxy interactions likely occur with high frequency, impact the H I properties of the cluster members even more severely: H I disks in galaxies located closest to the cluster core are more likely to be gas-deficient, truncated and asymmetrical. These trends are found even in loose clusters (Chamaraux et al. 1980; Haynes et al. 1985). Thus, peculiarities in the H I properties of a galaxy serve as a "fossil" record of past galaxy-galaxy interactions. Groups of galaxies which are dynamically evolved systems, whose members have experienced multiple disruptive interactions, would be expected to harbor a higher frequency of H I peculiarities. *Therefore, a comparative analysis of H I properties can be used as relative dynamical "age" indicator for groups of galaxies.*

Based on the idea that the neutral hydrogen properties is sensitive to environment, our main motivation for this single-dish H I line observational study of loose groups is to test whether "interacting" groups, which we define as groups hosting at least one pair of optically disturbed interacting galaxies, show evidence for prolonged histories of galaxy-galaxy interactions among the other group members. In the "interacting" groups, most of the galaxy members (with, of course, the exception of the interacting pair itself) show no unusual optical features indicative of past tidal interactions. Either (1) the group is a truly youthful kinematical system, having not yet experienced multiple tidal interactions within the system, or (2) the aftermath of previous galaxy-galaxy interactions among the other group members has left no signatures which are still optically visible. A comparative analysis of asymmetries in the H I line profile shapes (however with caution: see Richter & Sancisi 1994) and the total H I content for the galaxy groups can help distinguish between these two possibilities. Understanding the kinematical evolution of galaxy groups is particularly important, in light of HST observations of galaxy groups at very high redshift.

Though oft-cited H I mappings of galaxy groups frequently show tidal H I features, it would be misleading to draw the conclusion from these examples that such features are commonplace. Generally, these observations cover only the inner parts of groups, often centered on an interacting galaxy pair. Examples are the Arecibo maps of

groups by Haynes et al. (1981), showing tidal features from at least one group member in 6 of the 15 groups mapped, and the VLA maps of the M81 group by Yun et al. (1994). Observations searching for H I throughout the volume covered by groups are rare, due to the large apparent size of nearby groups. Systematic searches for H I clouds in groups were made at Arecibo by Lo & Sargent (1978) in the nearby M 81, NGC 1023 and CVnI groups (the latter was also covered in the Nançay blind H I line search by Kraan-Korteweg 1999) and by Zwaan (2000, 2000) in 6 groups at redshifts of 1800–3000 km s^{-1} (NGC 5798, 5962, 5970, 6278, 6500 and 6574) with properties similar to those of the Local Group of galaxies. All H I emission features detected in these searches could unambiguously be associated to optically identified galaxies or to a previously known H I tidal feature in the NGC 6500/01 pair. The 5σ H I mass detection limit for an H I cloud with a linewidth of 10 km s^{-1} is about 8×10^6 $M_\odot$ at the average distance of 30 Mpc (for $H_0 = 75$ km s^{-1} Mpc^{-1}) for the groups in Zwaans' study. For comparison, the detection limit of the present H I survey is about 4 times higher.

In this paper we present a new homogeneous set of H I 21-cm line observations for galaxies in 15 loose groups: 9 with at least one pair of strongly interacting galaxies and 6 without optical indicators of tidal interactions. The galaxy group sample selection is described in Sect. 2, where the basic optical properties of the program galaxies are listed as well. The observations and data reduction are described in Sect. 3, and the H I results are presented in Sect. 4, including notes to invidual galaxies for the interpretation of the 21-cm line data and a comparison of the observed global line parameters with published values. These H I data will, together with our optical and near-infrared data on the groups, provide the basis for a discussion of evolution within galaxy groups that is planned for a future paper (Marcum et al., in preparation).

2. The observed galaxy group sample

We used the Nançay telescope for a pencil beam H I line study of spiral galaxies and their surroundings in 15 loose groups. Program galaxies in our survey are members of groups selected from the Geller & Huchra (1983, GH83) group catalogue. Two different samples for comparison have been selected:

1. an "interacting" sample of 9 groups which were purposely chosen to contain at least one pair of strongly interacting Arp-type galaxies, as indicated by the presence of optical morphology peculiarities such as tidal tails;
2. a "control" sample of 6 groups with no optical indicators of gravitationally-induced tidal interactions between the group members.

An extensive optical (R and Hα) and near-infrared (J, H and K band) study has already been completed for this sample (Marcum 1994), providing a complementary data set to the H I radio observations. A multi-wavelength comparative analysis utilizing results from this Nançay H I data set is planned for a future paper.

The "interacting" group sample comprises 62 galaxies in 9 groups, of which 8 galaxies were not previously observed in H I and 4 were not detected. The "control" sample comprises 40 galaxies in 6 groups, of which 3 were not previously observed and 6 were not detected in the 21-cm line. Basic properties of the program objects are presented in Table 1.

Listed in the 7 columns of Table 1 are (1) Geller & Huchra (1983) group designation number; (2) total number of galaxy members in group; (3) right ascension and declination of the group, from Geller & Huchra (1983), converted from epoch B1950.0 to J2000.0; (4) mean recession velocity in km s^{-1} of the group members, using optical radial velocities from the LEDA database and corrected to the Galactic Standard of Rest, following de Vaucouleurs et al. (1991, hereafter RC3); (5) velocity dispersion of group, using mean optical radial velocities from the LEDA database; (6) adopted distance in Mpc, derived from the mean recession velocity of the group, corrected for Virgocentric infall, following LEDA, and using a Hubble constant of 75 km s^{-1} Mpc^{-1}; (7) total apparent B magnitude of group members, from Geller & Huchra (1983).

Tables 2 and 3 list basic optical properties of the target objects. The 9 columns of Tables 2 and 3 are: (1) GH83 group designation number; (2) galaxy identification; (3) right ascension and declination of the galaxy centroid, computed from data taken from RC3; (4) morphological type, from LEDA and NED; (5) apparent $B_{\rm T}$ magnitude, from LEDA; (6) galaxy isophotal B band diameter at the 25 mag arcsec^{-2} level, from LEDA; (7) axial ratio in the B band, from LEDA; (8) optical recessional velocity, from LEDA; (9) error in recessional velocity, from LEDA.

3. Observations and data reduction

During the period December 1997 – May 1999 we obtained 21-cm H I spectra for all sample group galaxies using the Nançay Decimetric Radio Telescope and autocorrelator spectrometer. The Nançay telescope is a meridian transit-type instrument with an effective collecting area of roughly 7000 m^2 (equivalent to a 94-m diameter parabolic dish). Due to the elongated geometry of the telescope, at 21-cm it has a half-power beam width of $3\farcm6$ E-W $\times$ $22'$ N-S for the range of declinations covered in this work (see Matthews & van Driel 2000). Tracking was generally limited to about 45 min per source per day. Typical system temperatures were $\sim$40 K. The Nançay beam is well suited for our project, since it will be sensitive to extended emission around group members which may have gone undetected with a smaller beam.

We obtained our observations in total power (position-switching) mode using consecutive pairs of two-minute on- and two-minute off-source integrations. Off-source integrations were taken at approximately $20'$ E of the target

Table 2. Basic optical data for the interacting group sample.

GH No. (1)	Ident. (2)	RA (2000.0) (3)	Dec.	Morphol. Class. LEDA	NED (4)	B_T mag (5)	D_{25} ($'$) (6)	axial ratio (7)	V_{opt} (km s^{-1}) (8)	err (km s^{-1}) (9)
45	NGC 2798*	09 17 22.9	42 00 02	SBa	SB(s)ap	13.03	2.7	0.35	1733	64
	NGC 2799*	09 17 31.4	41 59 39	SBm	SB(s)m?	13.96	1.8	0.29	1863	72
	NGC 2844	09 21 48.0	40 09 07	Sa	SA(r)a:	13.72	1.7	0.44	1495	16
	NGC 2852	09 23 14.2	40 09 53	SBa	SAB(r)a?	13.98	1.5	0.93	1821	54
58	NGC 3162	10 13 31.9	22 44 23	SBbc	SAB(rs)bc	12.20	3.1	0.83	1456	56
	NGC 3177	10 16 34.4	21 07 29	Sb	SA(rs)b	13.01	1.5	0.76	1220	56
	NGC 3185	10 17 38.6	21 41 19	SBa	(R)SB(r)a	12.82	1.7	0.6	1237	26
	NGC 3187	10 17 47.5	21 52 25	SBc	SB(s)cp	13.72	2.5	0.41	1582	28
	NGC 3189	10 18 05.7	21 49 59	Sa	SA(s)ap	11.86	4.6	0.42	1289	31
	NGC 3193	10 18 25.0	21 53 42	E	E2	11.70	2.2	0.9	1378	27
	NGC 3213	10 21 17.7	19 39 07	Sbc	Sbc:	14.13	1.0	0.79	1412	50
	NGC 3226*	10 23 27.4	19 53 55	E	E2:p	12.34	2.6	0.87	1325	72
	NGC 3227*	10 23 31.4	19 51 48	SBa	SAB(s)p	11.28	5.4	0.69	1145	54
	NGC 3239	10 25 05.5	17 09 35	Irr	IB(s)mp	11.71	4.5	0.54	830	52
67	UGC 5870	10 45 58.6	34 57 53	S0	S0?	14.27	1.1	1.00	2032	50
	NGC 3381	10 48 25.0	34 42 44	SBb	SBp	12.77	2.0	0.92	1506	33
	NGC 3395*	10 49 49.4	32 58 51	SBc	SAB(rs)cdp:	12.39	1.7	0.56	1634	39
	NGC 3396*	10 49 56.1	32 59 22	SBm	IBmp	12.48	2.7	0.42	1666	36
	NGC 3424	10 51 46.6	32 54 02	SBb	SB(s)b:?	13.07	2.7	0.28	1420	35
	NGC 3430	10 52 10.9	32 57 09	SBc	SAB(rs)c	12.21	4.1	0.55	1577	77
	NGC 3442	10 53 08.2	33 54 36	Sa	Sa?	13.80	0.6	0.77	1713	52
	UGC 6070	10 59 46.5	33 23 32	Sm	S?	13.45	0.7	0.77	1861	60
86	UGC 6545	11 33 44.5	32 38 04	SBb	S?	14.46	1.2	0.37	4278	1885
	NGC 3786*	11 39 42.4	31 54 35	SBa	SAB(rs)ap	13.44	2.0	0.55	2596	296
	NGC 3788*	11 39 44.0	31 55 58	SBab	SAB(rs)abp	13.33	1.6	0.26	2486	150
92	NGC 3902	11 49 18.9	26 07 22	SBbc	SAB(s)bc:	13.76	1.6	0.81	3628	50
	NGC 3920	11 50 06.3	24 55 15		S?	14.01	1.0	0.95	3611	37
	UGC 6806	11 50 19.7	25 57 42	Sc	Sp	14.17	1.9	0.32	3757	50
	NGC 3944	11 53 05.5	26 12 28	E-S0	S0-:	14.12	1.4	0.77	3638	31
	IC 746	11 55 34.6	25 53 19	Sbc	Sb	14.36	1.1	0.30	5000	50
	NGC 3987	11 57 21.2	25 11 41	Sb	Sb	13.90	2.2	0.19	4533	28
	NGC 3997	11 57 47.3	25 16 18	SBb	SBbp	14.02	1.6	0.55	4742	42
	NGC 4005	11 58 10.3	25 07 18	S?	Sb	13.89	1.2	0.59	4425	65
	NGC 4015A*	11 58 43.3	25 02 40	Sc	E	14.15	0.9	0.23	4780	57
	NGC 4015B*	11 58 43.1	25 02 35	Sab	S?	12.81	1.4	0.66	4347	44
	NGC 4022	11 59 01.1	25 13 19	S0	SAB0^0:	14.24	1.3	0.95	4340	88
126	NGC 5341	13 52 31.4	37 48 58	SBd	S?	14.08	1.3	0.42	3740	60
	NGC 5351	13 53 28.1	37 54 52	SBb	SA(r)b:	13.00	2.9	0.55	3845	66
	NGC 5378	13 56 50.6	37 48 00	SBa	(R')SB(r)a	13.67	2.7	0.83	3017	42
	NGC 5380	13 56 56.7	37 36 34	E-S0	SA0^-	13.26	1.9	1.00	3116	126
	NGC 5394*	13 58 33.8	37 27 18	SBb	SB(s)bp	13.69	1.7	0.66	3442	88
	NGC 5395*	13 58 38.3	37 25 32	Sb	SA(s)bp	12.12	2.6	0.53	3505	35
141	NGC 5529	14 15 34.1	36 13 36	Sc	Sc	12.74	6.5	0.11	2957	60
	NGC 5533	14 16 07.6	35 20 42	Sab	SA(rs)ab	12.70	3.2	0.60	3781	56
	NGC 5544*	14 17 02.4	36 34 21	S0-a	(R)SB(rs)0/a	13.97	1.1	0.89	3106	75
	NGC 5545*	14 17 05.4	36 34 34	Sbc	SA(s)bc:	14.90	1.0	0.34	3139	85
	NGC 5557	14 18 26.2	36 29 38	E	E1	11.91	2.3	0.79	3221	43
	NGC 5589	14 21 24.7	35 16 15	SBa	SBa	14.20	1.1	1.00	3391	50
	NGC 5590	14 21 38.0	35 12 19	S0	S0	13.42	1.8	1.0	3242	50
	NGC 5596	14 22 29.2	37 07 17	S0	S0	14.41	1.1	0.74	3265	351
	NGC 5614	14 24 08.2	34 51 27	Sab	SA(r)abp	12.54	2.4	0.83	3872	41
	NGC 5656	14 30 25.1	35 19 12	Sab	Sab	12.64	1.9	0.77	3150	9
	NGC 5675	14 32 39.8	36 18 12	SBb	S?	13.72	2.8	0.35	4066	108
	NGC 5684	14 35 49.8	36 32 35	S0	S0	13.59	1.6	0.85	4082	31
	NGC 5695	14 37 23.0	36 34 15	SBa	SBb	13.58	1.5	0.7	4168	115
153	NGC 5929*	15 26 05.5	41 40 17	Sa	Sab:p	14.06	1.0	0.95	2514	33
	NGC 5930*	15 26 07.8	41 40 39	SBab	SAB(rs)bp	13.53	1.8	0.46	2664	48
	UGC 9858	15 26 40.9	40 33 52	SBbc	SABbc	13.83	4.3	0.19	2624	8
156	NGC 5951	15 33 43.1	15 00 27	SBc	SBc:	13.47	3.6	0.22	1670	63
	NGC 5953*	15 34 32.4	15 11 42	S0-a	SAa:pec	13.13	1.8	0.74	2061	90
	NGC 5954*	15 34 34.8	15 12 12	SBc	SAB(rs)cd:p	13.12	1.3	0.48	2034	81
	NGC 5962	15 36 31.7	16 36 32	Sc	SA(r)c	12.03	3.0	0.72	1993	56

Note: Asterisks (*) in this and following tables denote target pairs which are confused within a single Nançay beam (see Table 6, also).

position. The autocorrelator was divided into two pairs of cross-polarized receiver banks, each with 512 channels and a 6.4 MHz bandpass. This yielded a channel spacing of 2.64 km s^{-1}, for an effective velocity resolution of ∼3.3 km s^{-1} at 21-cm, which was smoothed to a channel separation of 13.2 and a velocity resolution of 15.8 km s^{-1} during the data reduction, in order to search for faint features. The center frequencies of the two banks were tuned to the known redshifted H I frequency of the target. Total integration times were up to 5 hours per galaxy, depending on the strength of the source (see Tables 4 and 6).

We reduced our H I spectra using the standard DAC and SIR spectral line reduction packages available at the Nançay site. With this software we subtracted baselines (generally third order polynomials) and averaged the two receiver polarizations. To convert from units of $T_{\rm sys}$ to flux density in mJy we used the calibration procedure described in Matthews et al. (2000), see also Matthews et al. (1998) and Matthews & van Driel (2000). This procedure yields an internal calibration accuracy of about ±15% near the rest frequency of the 21cm line, where the observations presented here were made.

4. Results

Our reduced Nançay H I spectra are shown in Fig. 1. Integrated line fluxes, $I_{\rm HI}$, velocity widths at 50% and 20% of peak maximum, W_{50} and W_{20}, radial velocities, $V_{\rm HI}$ and rms noise levels of our new spectra were measured using standard Nançay reduction software for galaxy observations.

Derived Nançay H I profile parameters for the target galaxies are listed in Tables 4 and 6. For each group of galaxies, a single distance was assumed (see Table 1), calculated using a Hubble constant of 75 km s^{-1} Mpc^{-1} and the mean radial velocities of the group members, corrected for Virgocentric infall. No corrections have been applied to these values for, e.g., instrumental resolution or cosmological stretching (e.g., Matthews et al. 2000).

Listed in the 9 columns of Tables 4 and 6 are: (1) GH83 group designation number; (2) galaxy identification; (3) right ascension and declination of the galaxy centroid taken from the RC3; (4) recessional velocity, as derived from Nançay observations and corrected to the Galactic standard of rest, as well as its estimated uncertainty; (5) integrated neutral hydrogen line flux; (6) neutral hydrogen line full width measured at the 50% level of the peak flux density; (7) neutral hydrogen line full width measured at the 20% level of the peak flux density; (8) root-mean-square of the flux density, measured outside the emission line profile; (9) neutral hydrogen mass, using the adopted distance as given in Table 1; (10) luminosity in the B band, using the adopted distance as given in Table 1; (11) neutral hydrogen mass to B band luminosity ratio.

We estimated the uncertainties, $\sigma_{V_{\rm HI}}$, in the central H I velocities following Fouqué et al. (1990):

$$\sigma_{V_{\rm HI}} = 4R^{0.5}P_W^{0.5}X^{-1}\ [{\rm km\,s^{-1}}] \quad (1)$$

where R is the instrumental resolution (15.8 km s^{-1}), $P_W = (W_{20}-W_{50})/2$ [km s^{-1}] and X is the signal-to-noise ratio of a spectrum, which we defined as the ratio of the peak flux density and the rms noise. According to Fouqué et al., the uncertainty in the linewidths is $2\sigma_{V_{\rm HI}}$ for W_{50} and $3\sigma_{V_{\rm HI}}$ for W_{20}. The upper limits to the integrated H I line fluxes, $I_{\rm HI}$, are 3σ values for flat-topped profiles with a width of 300 km s^{-1}, a representative value for the galaxies detected.

4.1. Notes to individual galaxies

We searched the vicinity of the target objects for nearby spiral galaxies which could possibly give rise to confusion in those Nançay H I profiles where line emission was detected. We used the online NED and LEDA databases, in an area of 5.′5×30′ ($\alpha \times \delta$) about the pointing centre, i.e. about 1.5 times the HPBW, as well as optical images of a 24′ × 24′ area around each target galaxy extracted from the Digitized Sky Survey.

We have summarized previously-published results of single-dish H I observations as well as of interferometric H I line imaging of galaxies and groups from the sample (see also the catalogue of H I maps by Martin 1998). Global profile parameters derived from these data are given in Tables 6 and 7, where the following columns are listed, while the keys to the telescopes and references used in these two tables are given in Table 8:

(1) GH83 group designation number; (2) galaxy identification; (3) mean velocity of the H I line profiles; (4) integrated line flux of the H I profiles; (5) H I line width measured at the 50% level of the peak flux density; (6) H I line width measured at the 20% level of the peak flux density; (7) telescope used (see Table 8); (8) literature reference (see Table 8).

For some objects, extended H I emission may have been missed by the single Nançay profile pointed towards the galaxy's centre. To assess which H I masses may be underestimated, we have assumed the H I diameters to be 1.25 times as large the optical D_{25} dimensions, a rule-of-thumb from interferometric H I line imaging studies of normal, non-interacting spirals (e.g., Broeils & van Woerden 1994, and references therein). We have also noted other points of interest, like the presence of active nuclei.

4.1.1. Interacting group sample

Group GH 45:

NGC 2798/9 pair: our Nançay profile, like all other published single-dish profiles of the pair, is undoubtedly confused by H I emission from nearby spiral UGC 4904. VLA H I observations (Nordgren et al. 1997; see Table 6) show an integrated line flux of 7.0 Jy km s^{-1} and a mean velocity of about 1800 km s^{-1} for the pair, and 6.0 Jy km s^{-1} centered on 1670 km s^{-1} for UGC 4904. The pair shows an H I tail and signs of interaction in the velocity field; a total flux of about 5.0 Jy km s^{-1} resides in the two disks, and about 2.0 Jy km s^{-1} outside them.

Table 3. Basic optical data for the control group sample.

GH No. (1)	Ident. (2)	RA (2000.0) (3)	Dec.	Morphol. Class. LEDA	NED (4)	B_T mag (5)	D_{25} (′) (6)	axial ratio (7)	V_{opt} km s^{-1} (8)	err km s^{-1} (9)
49	NGC 2998	09 48 43.6	44 04 52	SBc	SAB(rs)c	13.10	2.9	0.48	4767	19
	NGC 3009	09 50 10.5	44 17 40	Sc	S?	13.36	0.8	0.93	4604	50
	UGC 5295	09 52 54.1	42 50 55	SBb	SAB(s)b	14.26	2.1	0.56	4805	40
57	NGC 3156	10 12 41.1	03 07 50	S0	SO:	13.07	1.9	0.62	1230	89
	NGC 3165	10 13 31.4	03 22 32	Sm	SA(s)dm	14.49	1.4	0.49	1317	50
	NGC 3166	10 13 44.9	03 25 31	S0-a	SABO$^-$a	11.22	4.7	0.46	1329	75
	NGC 3169	10 14 14.3	03 28 08	Sa	SA(s)ap	11.04	4.6	0.56	1253	46
89	UGC 6617	11 39 17.5	09 57 48	S0	S0?	14.28	0.9	0.36	6228	31
	NGC 3817	11 41 53.1	10 18 07	S0-a	SB0/a	14.27	0.7	0.76	6102	32
	NGC 3822*	11 42 11.3	10 16 40	S0	Sb	14.10	0.8	0.60	6132	33
	NGC 3825*	11 42 23.7	10 15 52	SBa	SBa	13.93	0.9	0.81	6436	132
	IC 724	11 43 34.7	08 56 31	Sa	Sa	13.49	2.3	0.40	5959	16
	NGC 3843	11 43 54.1	07 55 32	S0-a	S0/a	14.00	1.0	0.45	5908	50
	NGC 3839	11 43 54.4	10 46 59	Sd	Sdm:	13.60	1.0	0.51	5920	45
118	NGC 5141	13 24 51.6	36 22 40	S0	S0	13.80	1.7	0.76	5201	101
	NGC 5142	13 25 01.3	36 23 58	S0	S0	14.20	1.3	0.67	5235	65
	NGC 5149	13 26 09.7	35 56 04	SBbc	SBbc	13.90	1.5	0.64	5601	49
123	NGC 5289	13 45 09.2	41 30 11	SBab	(R)SABab:	13.95	1.6	0.31	2446	51
	NGC 5290	13 45 19.2	41 42 55	Sbc	Sbc:	13.29	3.7	0.27	2544	48
	NGC 5297	13 46 24.1	43 52 25	SBc	SAB(s)c:	12.39	5.5	0.23	2492	106
	NGC 5311	13 48 55.9	39 59 07	S0-a	S0/a	13.59	2.6	0.81	2698	40
	UGC 8736	13 49 03.9	39 29 56	Sc	S?	14.25	1.3	0.42	2404	50
	NGC 5313	13 49 44.7	39 59 10	Sb	Sb?	12.71	1.7	0.56	2597	44
	NGC 5320	13 50 20.5	41 22 06	SBc	SAB(rs)c:	12.96	3.6	0.49	2646	65
	NGC 5326	13 50 50.7	39 34 29	Sa	SAa:	12.90	2.2	0.54	2540	68
	NGC 5336	13 52 10.9	43 14 34	Sc	Scd:	13.57	1.4	0.89	2297	60
	NGC 5337	13 52 23.1	39 41 15	S?	S?	13.35	1.7	0.48	2208	46
	NGC 5350*	13 53 21.5	40 21 48	SBbc	SB(r)b	12.23	2.7	0.80	2322	61
	NGC 5354*	13 53 26.6	40 18 16	S0	E2	12.40	1.7	0.87	2681	244
	NGC 5353	13 53 26.8	40 17 03	S0	S0	11.97	1.9	0.71	2170	103
	NGC 5355	13 53 45.9	40 20 17	S0	E3	13.98	0.6	0.64	2422	38
	NGC 5362	13 54 53.5	41 18 51	Sb	Sb?p	13.20	2.2	0.44	2228	45
	NGC 5371	13 55 40.5	40 27 44	SBbc	SAB(rs)bc	11.38	4.2	0.81	2570	40
	NGC 5383	13 57 05.2	41 50 44	SBb	(R')SB(rs)b:p	12.10	2.7	0.81	2227	26
155	NGC 5934	15 28 12.4	42 55 49	S?	S?	14.60	0.7	0.47	5600	39
	NGC 5945	15 29 45.2	42 55 14	SBab	SB(rs)ab	13.80	2.6	0.85	5521	50
	IC 4562	15 35 57.6	43 29 40	E	E?	13.81	1.2	1.00	5666	145
	IC 4564*	15 36 27.0	43 31 08	Sc	S?	14.41	1.3	0.35	5669	39
	IC 4566*	15 36 42.6	43 32 24	Sab	Sab	14.11	1.6	0.64	5608	47
	IC 4567	15 37 13.3	43 17 54	Sc	Scd?	13.51	1.4	0.71	5775	40

Note: Asterisks (*) in this and following tables denote target pairs which are confused within a single Nançay beam (see Table 7, also).

Group GH 58:

NGC 3162: Four of the six available integrated line fluxes of this object are in agreement (∼26 Jy km s^{-1}), the exceptions being the considerably higher Nançay value (44.1 Jy km s^{-1}) of Bottinelli et al. (1982) and the considerably lower (6.2 Jy km s^{-1}) Arecibo value of Williams & Rood (1987), whose W_{20} of 605 km s^{-1} is about three times larger than the other available values.

NGC 3177: The 2 Nançay and the 3 Arecibo I_{HI} measurements are about equally divided around two values

(5.9 and 3.3 Jy km s^{-1}) without consistency per telescope. This excludes a possible beam size effect and, in any case, the H I diameter of this galaxy with its 1.′5 D_{25} diameter is not expected to exceed the beam size of either telescope.

NGC 3185/87/89/93 subgroup: the area covering NGC 3185/87/89/93 was mapped in H I at the VLA by Williams et al. (1991), who, erroneously, refer to NGC 3189 as NGC 3190. These data show that our NGC 3185 spectrum will be confused by emission from NGC 3187 in the ∼1300–1400 km s^{-1} range, and that our NGC 3187 and NGC 3189 spectra will be confused by each other in the ∼1400–1500 km s^{-1} range. The Nançay pointings should cover essentially all emission from NGC 3187 and 3189, judging from the VLA H I column density map. The H I line flux we measured towards NGC 3187 (8.8 Jy km s^{-1}) is comparable to the value of 10.6 Jy km s^{-1} measured at the VLA for this object, though on average two times lower than the previously published Nançay values (24.6: and 14.2 from, respectively, Bottinelli et al. 1982; Balkowski & Chamaraux 1983). The uncertain integrated H I line flux of NGC 3189 measured at Green Bank (7.3: Jy km s^{-1}, Huchtmeier 1982) and the Arecibo measurement of 6.1 by Krumm & Salpeter (1982) are about twice as large as our Nançay value (3.1). Our value is consistent, however, with the mean of the four other literature values, 3.5 Jy km s^{-1}. NGC 3185 is an (R)SB(r)a with a Seyfert2 spectrum, and NGC 3189 an SA(s)apec with a LINER spectrum.

NGC 3226/7 pair: mapped in H I at the VLA (Mundell et al. 1995). No H I was detected in NGC 3226, and NGC 3227 shows a complex H I distribution and kinematics. About half the H I resides in a disk with a normal rotation curve, the rest in two plumes extending 7′ N and 16′ S of the system, and in an H I feature at the base of the N plume which may be a gas-rich dwarf galaxy. As the plumes have a N-S orientation, the Nançay beam will cover almost all of the H I emission, as the southernmost half of the southern plume is relatively faint compared to the bulk of the emission. Our Nançay integrated line flux (16.6 Jy km s^{-1}) is consistent with the Green Bank and Jodrell Bank data, while the Arecibo values are a bit lower. The only significantly discrepant Arecibo value is the 6.8 Jy km s^{-1} from Chamaraux et al. (1987). Our W_{20} profile width is consistent with the other measurements, but our W_{50} value (103 km s^{-1}) is similar to the Green Bank measurement by Peterson (1979) only, the 5 other published values are ∼350 km s^{-1} on average. NGC 3226 is an E2:pec with a LINER spectrum, and NGC 3227 an SAB(s)pec with a Seyfert1.5 spectrum.

NGC 3239: Four small galaxies will be included in the Nançay beam centered on this nearby (V = 830 km s^{-1}) irregular galaxy. Three of these have been previously catalogued, two (CGCG 094-039 and CGCG 094-043) with optical redshifts (Falco et al. 1999) around 13,300 km s^{-1}, and another, CGCG 094-040, without known redshift. The latter, faint (B_T 15.3 mag) object of less than 1′ diameter, is not expected to cause confusion with the very strong (75 Jy km s^{-1}) H I detection of NGC 3239. The nearby companions may well explain the much higher H I line flux measured at Green Bank (∼80 Jy km s^{-1} on average), compared to the Nançay and Arecibo values (43–61 Jy km s^{-1}) – see Table 6. In principle, some H I emission from NGC 3239 may fall outside the Nançay beam, as its optical E-W D_{25} diameter of 4.′5 exceeds the 3.′6 E-W HPBW, and as it looks like the result of a recent merger, which might have H I plumes associated with it, not covered by the Nançay beam.

Group GH 67:

UGC 5870: we registered an off-band detection of a galaxy at V = 1616 km s^{-1}, with a $FWHM$ = 120 km s^{-1}. This detection does not appear to disturb the detection of the target galaxy, which shows a classical double-horned spectrum.

NGC 3381: The integrated line flux of 21 Jy km s^{-1} measured at Arecibo by Krumm & Salpeter (1980) is the result of a crude mapping of the galaxy's H I distribution; a lower limit of 10′ is given by the authors for the H I diameter, indicating that the actual extent exceeds the mapped area. The other available I_{HI} values (8.5–13 Jy km s^{-1}) underestimate the total line flux. No galaxies that could be potential sources of confusion were found in a 24′ × 24′ area centered on the object.

NGC 3395/96: this pair was mapped in H I at the VLA (Clemens et al. 1999). An integrated flux of 22 Jy km s^{-1} was detected in the pair, which shows a clear H I bridge, as well as 4 Jy km s^{-1} in an H I tail extending to a distance of 10′ SW of the pair. The H I kinematics were modeled by the authors using N-body simulations, which indicate that the tail was stripped from NGC 3395. The Nançay and Arecibo line fluxes agree well, and are about two times smaller than the 38.4 Jy km s^{-1} was at Green Bank by Shostak (1975).

NGC 3424 and NGC 3430: our Nançay profiles of these two nearby objects (4.′5 E-W separation) will be mutually confused by their line emission, as will the published Green Bank and Jodrell Bank profiles of NGC 3430. The Arecibo profiles (Helou et al. 1982) of the two galaxies are not expected to be confused, given the telescope's small HPBW. The Arecibo central velocities are 1501/1586 km s^{-1}, the $FWHM$s 353/340 km s^{-1}, and the integrated line fluxes 14.0/44.1 Jy km s^{-1}, respectively.

NGC 3442: our Nançay profile parameters agree well with those of 4 of the 5 available Arecibo profiles; the integrated line flux measured at Arecibo by Magri (1994) is about 3 times larger (9.1 Jy km s^{-1}), though the profile's central velocity and linewidth are consistent the other measurements.

Group GH 86:

UGC 6545: for this object two completely discrepant optical redshifts have been published: 2619 ± 41 km s^{-1}, a CfA redshift value (Huchra et al. 1983; Huchra et al. 1995) and 6419 ± 90 km s^{-1} (Karachentsev 1980). Our Nançay value, 2630 km s^{-1}, is consistent with the Huchra et al. value.

Table 4. Nançay H I line data for the interacting group sample.

GH	Ident.	RA	Dec.	$V_{\rm HI}$	$I_{\rm HI}$	W_{50}	W_{20}	rms	$M_{\rm HI}$ [log]	L_B [log]	$M_{\rm HI}/L_B$
No.	No.	(2000.0)		km s^{-1}	Jy km s^{-1}	km s^{-1}	km s^{-1}	mJy	$M_\odot$	$L_{\odot,B}$	$M_\odot/L_{\odot,B}$
45	N2798/9*	09 17 27	41 59 50	1750 ± 8	10.9	304	424	2.7	9.18	9.90	0.19
	N2844	09 21 48	40 09 07	1494 ± 4	7.6	309	337	2.8	9.03	9.48	0.35
	N2852	09 23 14	40 09 53	1781 ± 3	5.2	211	232	2.1	8.86	9.37	0.31
58	N3162	10 13 32	22 44 23	1301 ± 2	25.6	183	204	5.9	9.27	9.80	0.30
	N3177	10 16 35	21 07 29	1326 ± 16	3.4	180	325	3.3	8.39	9.48	0.08
	N3185	10 17 39	21 41 19	1225 ± 6	3.1	248	276	2.5	8.35	9.55	0.06
	N3187	10 17 48	21 52 25	1589 ± 11	8.8	236	296	5.5	8.81	9.19	0.41
	N3189	10 18 06	21 49 53	1300 ± 23	5.0	458	560	4.4	8.56	9.94	0.04
	N3193	10 18 25	21 53 42	1361 ± 25	1.5	470	514	2.2	8.05	10.00	0.01
	N3213	10 21 18	19 39 07	1345 ± 13	1.3	149	187	2.4	7.97	9.03	0.09
	N3226/7*	10 23 30	19 52 51	1146 ± 5	16.6	103	437	2.3	9.08	10.31	0.06
	N3239	10 25 06	17 09 35	762 ± 1	43.3	132	183	3.5	9.50	10.00	0.32
67	U5870	10 45 59	34 57 53	1992 ± 4	4.6	229	244	2.9	8.80	9.25	0.35
	N3381	10 48 25	34 42 44	1629 ± 2	13.0	68	135	3.5	9.25	9.85	0.25
	N3395/6*	10 49 53	32 59 06	1637 ± 2	18.1	105	180	2.6	9.40	10.29	0.13
	N3424	10 51 47	32 54 02	1507 ± 5	15.5	318	401	2.8	9.33	9.73	0.40
	N3430	10 52 11	32 57 09	1584 ± 2	30.7	333	353	3.9	9.63	10.07	0.36
	N3442	10 53 08	33 54 36	1731 ± 5	3.2	133	160	2.1	8.64	9.44	0.16
	U6070	10 59 47	33 23 32	1853 ± 5	5.2	115	157	2.9	8.85	9.58	0.19
86	U6545	11 33 45	32 38 04	2630	1.0	150:		2.5	8.53	9.55	0.10
	N3786/8*	11 39 43	31 55 16	2674 ± 7	14.1	436	535	2.3	9.57	10.28	0.19
92	N3902	11 49 19	26 07 22	3651 ± 11	8.9	241	371	4.5	9.85	10.22	0.43
	N3920	11 50 06	24 55 15	3635 ± 3	8.4	181	211	2.9	9.82	10.12	0.51
	U6806	11 50 20	25 57 42	3751 ± 2	17.5	205	245	2.8	10.14	10.05	1.24
	N3944	11 53 06	26 12 28	—	<3.1	—	—	3.4	<9.39	10.07	<0.21
	I746	11 55 35	25 53 19	5027 ± 6	6.7	268	288	3.9	9.73	9.97	0.57
	N3987	11 57 21	25 11 41	4450 ± 7	7.8	521	551	2.3	9.79	10.16	0.43
	N3997	11 57 47	25 16 18	4771 ± 5	7.6	241	273	3.2	9.78	10.11	0.47
	N4005	11 58 10	25 07 18	—	<2.3	—	—	2.6	<9.27	10.16	<0.13
	N4015A/B*	11 58 43	25 02 35	4516 ± 25	3.1	404	524	3.1	9.39	10.70	0.05
	N4022	11 59 01	25 13 19	—	<2.6	—	—	2.9	<9.34	10.02	<0.20
126	N5341	13 52 32	37 48 58	3649 ± 4	5.1	252	265	3.1	9.42	9.91	0.33
	N5351	13 53 28	37 54 52	3607 ± 4	18.3	415	438	5.1	9.98	10.34	0.44
	N5378	13 56 51	37 48 00	3000 ± 22	3.9	301	367	5.0	9.31	10.07	0.17
	N5380	13 56 57	37 36 34	3000 ± 11	2.9	304	336	2.5	9.18	10.23	0.09
	N5394/5*	13 58 36	37 26 25	3454 ± 12	20.0	457	577	5.4	10.02	10.78	0.17
141	N5529	14 15 34	36 13 36	2884 ± 3	26.4	565	604	3.1	10.17	10.49	0.48
	N5533	14 16 08	35 20 42	3864 ± 2	19.3	431	456	2.7	10.04	10.49	0.35
	N5544/5*	14 17 04	36 34 28	3071 ± 14	3.8	247	310	2.9	9.33	10.14	0.16
	N5557	14 18 26	36 29 38	—	<2.6	—	—	2.9	<9.17	10.81	<0.02
	N5589	14 21 25	35 16 15	3397 ± 8	1.3	182	195	2.2	<8.20	9.89	0.10
	N5590	14 21 38	35 12 19	—	<2.8	—	—	3.1	<8.96	10.21	<0.10
	N5596	14 22 29	37 07 17	3122 ± 13	1.0	544	554	3.4	8.75	9.81	0.09
	N5614	14 24 08	34 51 27	3893 ± 12	3.2	138	246	2.3	9.26	10.56	0.05
	N5656	14 30 25	35 19 12	3163 ± 6	8.2	338	377	3.2	9.67	10.52	0.14
	N5675	14 32 40	36 18 12	—	<2.2	—	—	2.4	<9.09	10.09	<0.10
	N5684	14 35 50	36 32 35	—	<2.3	—	—	2.6	<9.12	10.14	<0.10
	N5695	14 37 23	36 34 15	—	<2.4	—	—	2.7	<9.13	10.14	<0.10
153	N5929/30*	15 26 07	41 40 28	2539 ± 14	3.0	219	299	2.3	8.96	10.13	0.07
	U9858	15 26 41	40 33 52	2621 ± 2	30.5	364	388	2.6	10.00	9.80	1.57
156	N5951	15 33 43	15 00 27	1780 ± 1	17.5	265	284	1.6	9.48	9.67	0.65
	N5953/4*	15 34 33	15 11 57	1966 ± 4	7.7	146	275	1.9	9.13	9.81	0.21
	N5962	15 36 32	16 36 32	1957 ± 2	17.6	341	364	2.3	9.49	10.25	0.17

NGC 3786/8: short Westerbork synthesis observations of the pair were obtained by Oosterloo & Shostak (1993), but they refrain from listing global line parameters as NGC 3786 (= UGC 6621) is "not detected or confused with NGC 3788 (= UGC 6623)", and NGC 3788 is "possibly confused with NGC 3786". Their Arecibo observations of the pair were confused as well and no single-dish profile parameters are given. Our Nançay integrated line flux (14.1 Jy km s^{-1}) is similar to the Green Bank value, and both are about 1.5 times larger than 4 of the 5 available Arecibo values, the exception being the much lower (4.9 Jy km s^{-1}) measurement by Lewis et al. (1985). NGC 3786 is an SAB(rs)apec with a Seyfert1.8 spectrum.

Group GH 92:

UGC 6806: our Nançay profile will be confused by nearby UGC 6807, a $B_{\rm T}$ 15.0 mag Irregular at 2′ separation. Even the Arecibo profile of UGC 6806 (Williams 1986, see Table 6) should be confused, as their HPBW is about the same as the galaxies' separation. The Nançay integrated line flux (17.5 Jy km s^{-1}) is 4 times higher than the Arecibo value, though the central velocities and profile widths are quite similar. For UGC 6807, only a Nançay

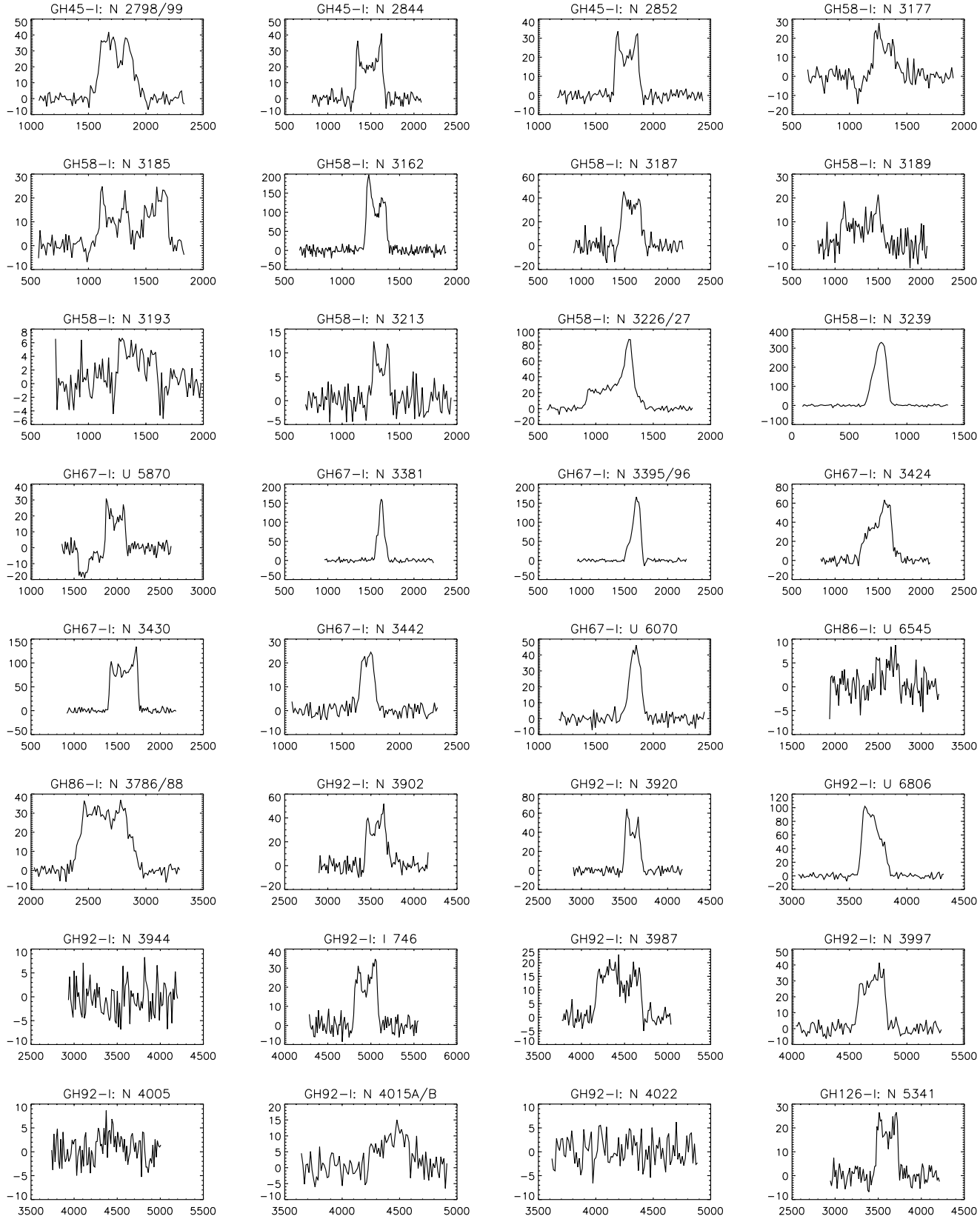

Fig. 1. a) Nançay 21-cm H I line spectra. Each galaxy is identified by its GH group number, followed by an "I" for the interacting sample or a "C" for the control sample, and its individual catalog identification. The velocity resolution of the spectra is 15.8 km s^{-1}. The axes are heliocentric velocity (in km s^{-1}) and flux density (in mJy).

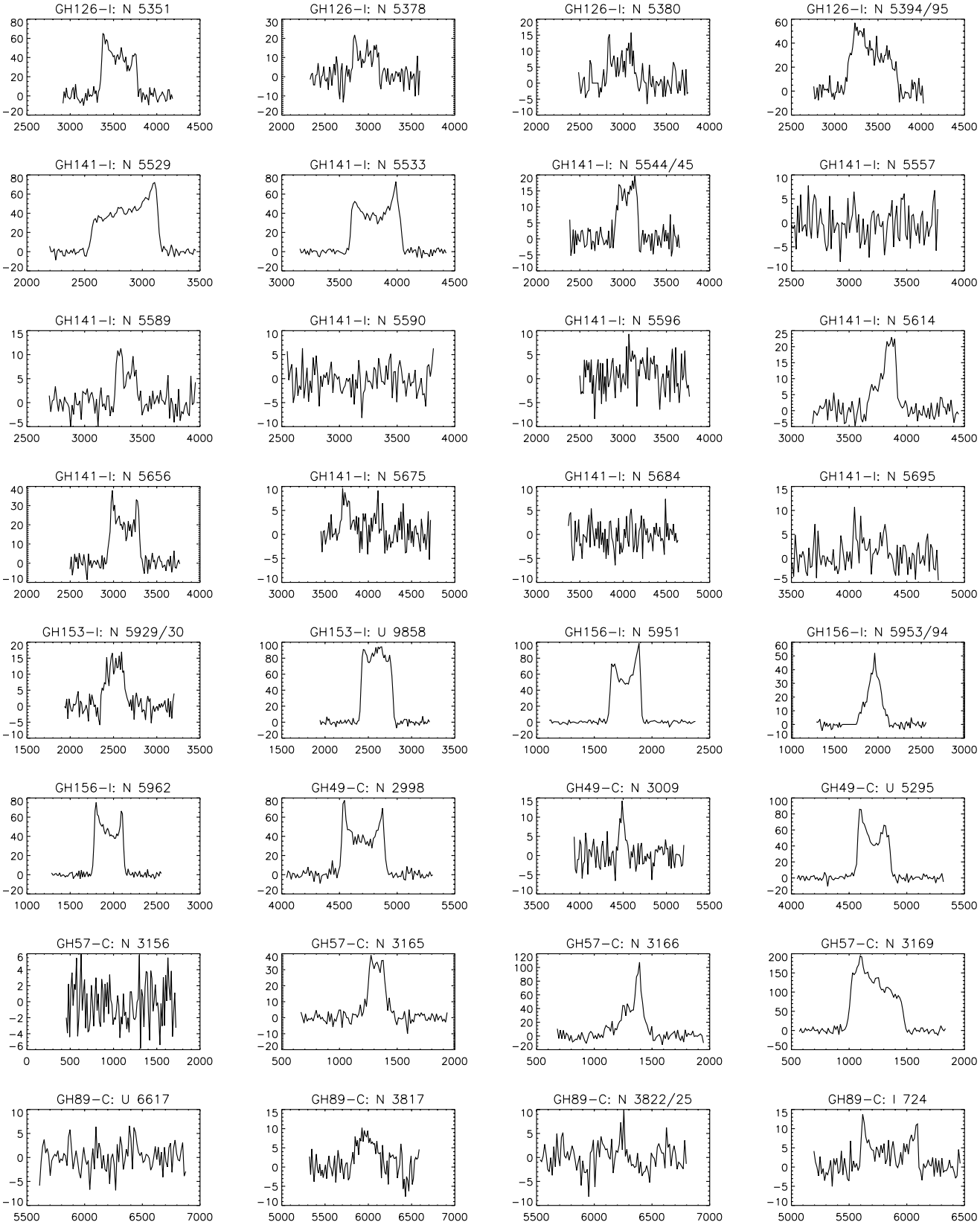

Fig. 1. b) continued.

profile pointed at UGC 6807 is available in the literature (Garcia et al. 1994), which will be confused by UGC 6806. In conclusion, no reliable H I profiles of these two objects are available.

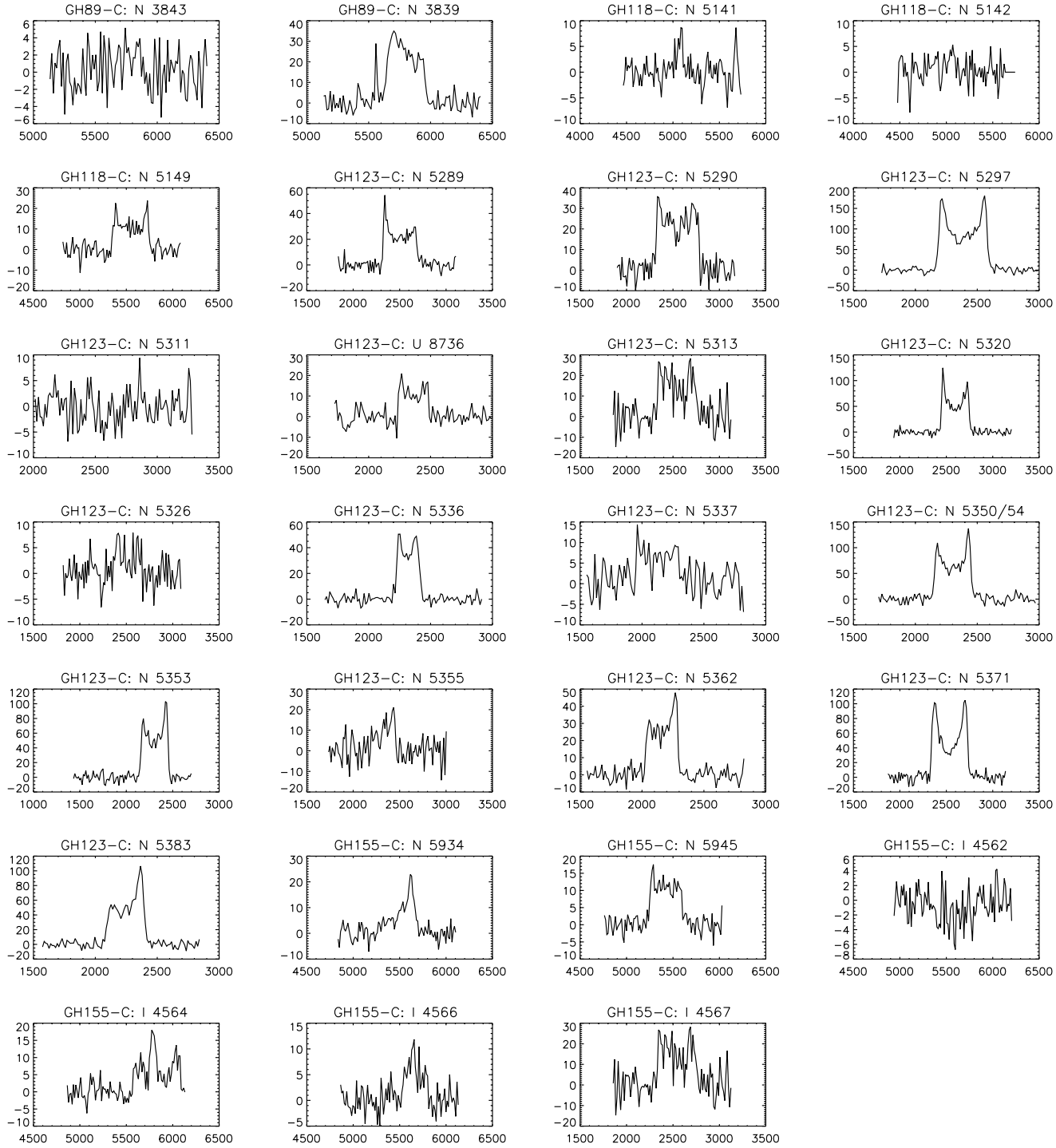

Fig. 1. c) continued.

NGC 3944: E/S0 galaxy, not detected in our survey (estimated $I_{\rm HI} < 3.1$ Jy km s^{-1}, $M_{\rm HI}/L_B < 0.21\ M_\odot/L_{\odot,B}$).

NGC 3987: Our H I velocity is about 50 km s^{-1} lower than the 4 reported Arecibo values, and all profiles have very large widths. The mean values for the Arecibo spectra of NGC 3987 are $V_{\rm HI} = 4500$ km s^{-1}, $W_{20} = 569$ km s^{-1} and $I_{\rm HI} = 7.1$ Jy km s^{-1}. A possible source of confusion is the $B_{\rm T}$ 15.8 mag Sbc spiral NGC 3989, at an E-W distance of 1′.2 from NGC 3987. NGC 3989 has no published optical redshift. The Arecibo H I profile parameters for NGC 3989 of Mould et al. (1993) and Scodeggio et al. (1993 – where NGC 3987 is referred to as NGC 3997) are comparable (average $V_{\rm HI} = 4623$ km s^{-1}, $W_{20} = 519$ km s^{-1} and $I_{\rm HI} = 3.2$ Jy km s^{-1}), while the Arecibo profile of Williams (1986) has a 90 km s^{-1} higher central velocity (4713 km s^{-1}), less flux (2.0 Jy km s^{-1}) and a considerably smaller width ($W_{20} = 374$ km s^{-1}). Confusion between the Arecibo profiles of NGC 3987 and 3989 is in principle possible, as their projected separation is 2′.6;

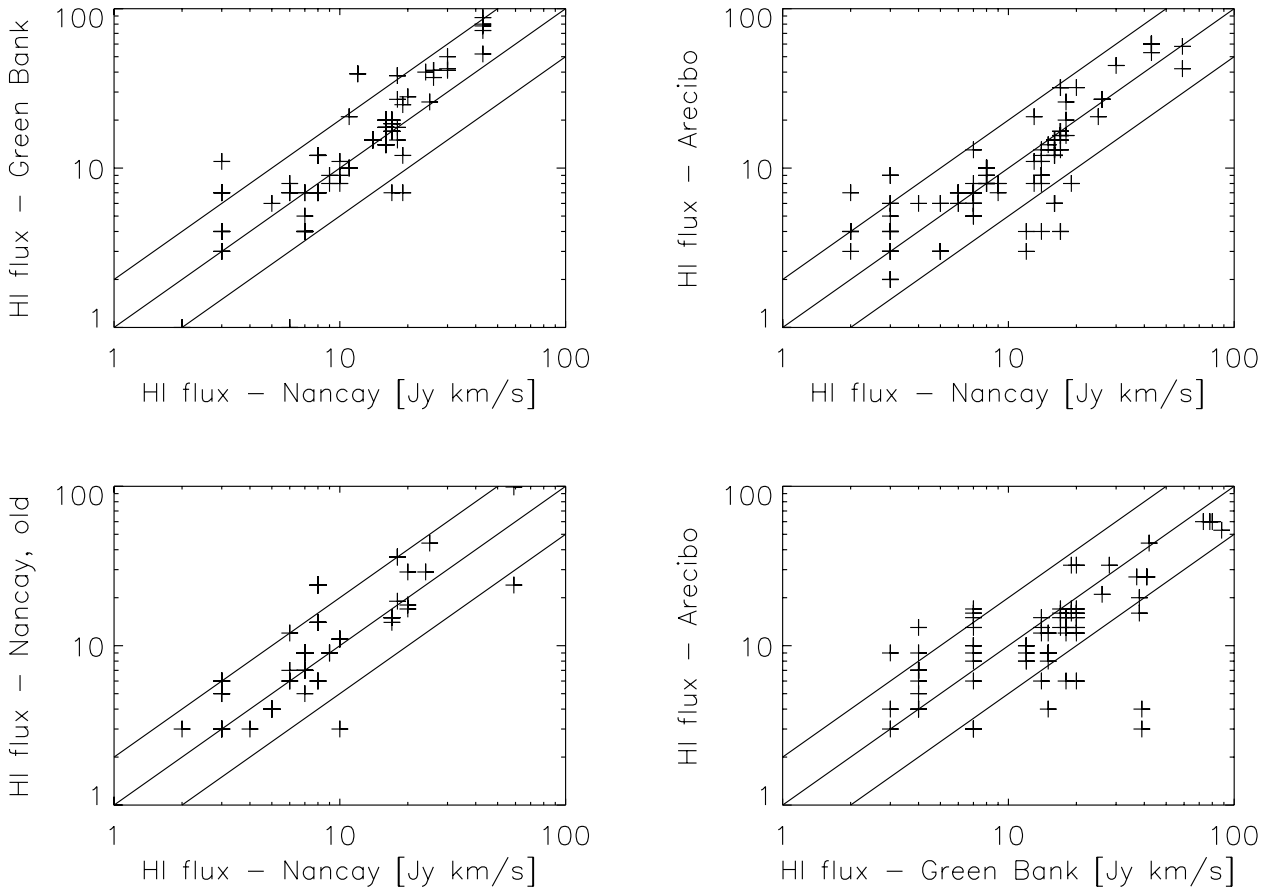

Fig. 2. Comparison of integrated H I line fluxes measured for the present Nançay survey with literature values (see Tables 7 and 8): Green Bank, Arecibo and Nançay, as well as between the literature Green Bank and Arecibo values. Three diagonal lines have been plotted in each panel: the middle line has a slope of unity, the upper line indicates a two times higher flux measured elsewhere than was measured at Nançay, and the lower line a two times lower flux than measured at Nançay. These lines are not fits to the data, they merely serve to guide the eye.

in fact, the spectrum of Scodeggio et al. has a complex structure, indicative of confusion or interaction. On the other hand, the H I emission observed at Arecibo towards NGC 3989 cannot explain the H I observed at Nançay towards NGC 3987 below the low-velocity edge of the Arecibo profile of NGC 3987. In conclusion, the H I distribution appears complex and extended tidal debris may be present in H I.

NGC 3997: our Nançay profile ($V_{\rm HI}$ = 4771 km s^{-1}, W_{20} = 241 km s^{-1}, $I_{\rm HI}$ = 7.6 Jy km s^{-1}) can in principle be confused by two galaxies: NGC 3993, a $B_{\rm T}$ 14.2 mag Sbc spiral with $V_{\rm opt} = 4824 \pm 58$ km s^{-1} (LEDA) 2.′3 west of NGC 3997 and NGC 4000, a $B_{\rm T}$ 15.2 mag Sbc spiral without known $V_{\rm opt}$, 1.′9 east of NGC 3997. Arecibo observations with a HPBW of 3.′3 are available of all three galaxies. These will certainly resolve the confusion between NGC 3997 and NGC 4000 (7.′9 separation) and in principle between NGC 3997 and NGC 3993 (2.′8 separation) as well. Measured at Arecibo, the H I profile parameters of NGC 3997 are V = 4768 km s^{-1}, W_{20} = 289 km s^{-1}, $I_{\rm HI}$ = 7.9 Jy km s^{-1} (Gavazzi 1987; Williams 1986), those of NGC 3993 are V = 4826 km s^{-1}, W_{20} = 382 km s^{-1}, $I_{\rm HI}$ = 4.3 Jy km s^{-1} (Dell'Antonio et al. 1996; Williams 1986), and those of NGC 4000 are V = 4556 km s^{-1}, W_{20} = 310 km s^{-1}, $I_{\rm HI}$ = 2.3 Jy km s^{-1} (Gavazzi 1987; Williams 1986).

NGC 4005: Sb spiral, not detected clearly in our survey (estimated $I_{\rm HI} < 2.3$ Jy km s^{-1}). The 3 published Arecibo detections have almost the same integrated line flux as our estimated 3σ upper limit ($\sim$1.8 Jy km s^{-1}).

NGC 4015A/B: very close pair, with only 0.′4 separation between the nuclei; NGC 4015 is seen face-on, while NGC 4015 B is seen edge-on. Their optical redshifts are 4780 ± 57 and 4347 ± 44 km s^{-1}, respectively. Both the Arecibo and the Effelsberg spectra (Williams 1986; Huchtmeier et al. 1995) show two distinct peaks, centered on $\sim$4100 and $\sim$4500 km s^{-1}, respectively. In both papers the global line parameters listed refer to the entire emission line profile, resulting in very large W_{20} linewidths of 700–815 km s^{-1}. In our spectrum, only the emission centered on 4500 km s^{-1} is present. Huchtmeier et al. considered their profile confused by nearby spirals, but there are no candidates for confusion in the Arecibo or Nançay beams. The origin of the H I emission at 4100 km s^{-1} is unclear, but could be related to tidal debris.

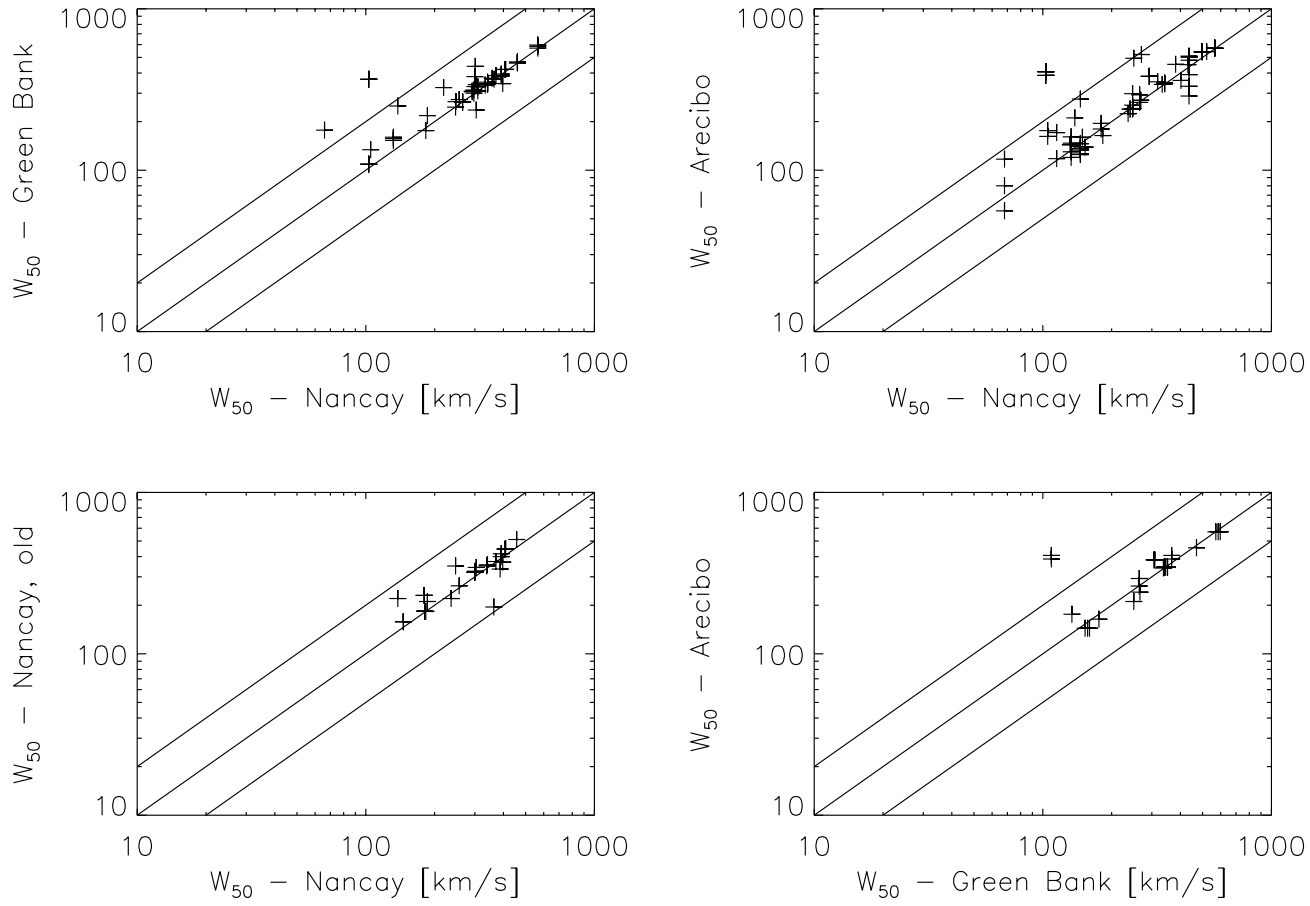

Fig. 3. Comparison of W_{50} H I line widths measured for the present Nançay survey with literature values (see Tables 7 and 8): Green Bank, Arecibo and Nançay, as well as between the literature Green Bank and Arecibo values. Three diagonal lines have been plotted in each panel: the middle line has a slope of unity, the upper line indicates a two times larger W_{50} measured elsewhere than was measured at Nançay, and the lower line a two times smaller W_{50} than measured at Nançay. These lines are not fits to the data, they merely serve to guide the eye.

NGC 4022: S0 galaxy, not detected in our survey (estimated $I_{\rm HI} < 2.6$ Jy km s^{-1}, $M_{\rm HI}/L_B < 0.20\, M_\odot/L_{\odot,B}$).

Group GH 126:

NGC 5351: short Westerbork H I synthesis observations (Rhee & van Albada 1996) show an H I diameter of 4′.0 at a surface density level of 1 $M_\odot$ pc^{-2}, 1.4 times the optical D_{25} diameter. Though the H I major axis diameter somewhat exceeds the Nançay 3′.6 E-W HPBW, all measured integrated line fluxes are in agreement and no significant flux seems to have been missed in our survey.

NGC 5378 and 5380: in principle, our Nançay profiles of these two galaxies are expected to be mutually confused, as they are separated by 11′.4 (about half a HPBW) in the N-S direction. As NGC 5380 has been classified as an elliptical/S0 in various catalogues, we do not expect to detect it in H I; an upper limit of 1.26 Jy km s^{-1} was reported for NGC 5380 at Arecibo (Chamaraux et al. 1987), where the 3′.6 HPBW should not cause any confusion with NGC 5378. In fact, our detections towards the centres of both objects show strikingly similar profile parameters, indicating they are in fact both detections of the spiral NGC 5378. For their Nançay profile, Theureau et al. (1998), who assumed it to be confused with NGC 5380, listed only a central velocity (2715 km s^{-1}), which is about 260 km s^{-1} lower than that of the other two spectra. However, our measurement of the central H I velocity from the spectrum of Theureau et al. is 2990 km s^{-1}, in agreement with the other two spectra, and the linewidths we measured from their spectrum (see Table 6) are in agreement with our Nançay values. The integrated line flux we estimated from the plotted spectrum, ∼3.9 Jy km s^{-1}, is in also agreement with our value. Therefore, only the values measured by us from the Theureau et al. spectrum have been listed in Table 6. On the other hand, the line flux of NGC 5378 measured at Green Bank by Richter & Huchtmeier (1991), 11.2 Jy km s^{-1}, is much higher than the Nançay values and their profile widths about 40% larger. This Green Bank profile is not expected to be confused by NGC 5380, given the telescope's HPBW, nor are any other galaxies visible in its vicinity. A broad

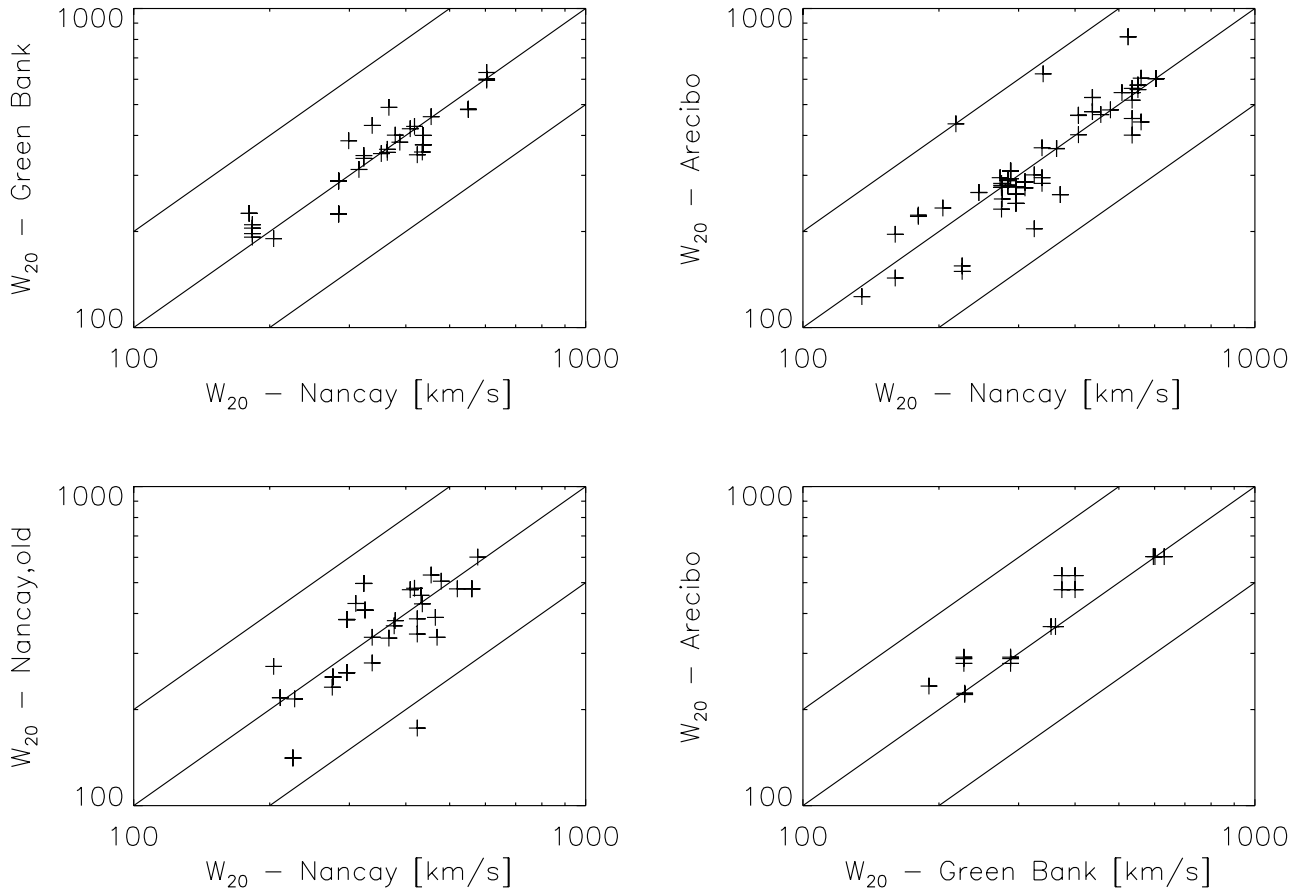

Fig. 4. Comparison of W_{20} H I line widths measured for the present Nançay survey with literature values (see Tables 7 and 8): Green Bank, Arecibo and Nançay, as well as between the literature Green Bank and Arecibo values. Three diagonal lines have been plotted in each panel: the middle line has a slope of unity, the upper line indicates a two times larger W_{20} measured elsewhere than was measured at Nançay, and the lower line a two times smaller W_{20} than measured at Nançay. These lines are not fits to the data, they merely serve to guide the eye.

RFI signal seems the only plausible cause of the striking discrepancy between the Green Bank and Nançay profiles.

Group GH 141:

NGC 5529: short Westerbork H I synthesis observations (Rhee & van Albada 1996) show an H I diameter of 6.′6 at a surface density level of 1 $M_\odot$ pc^{-2}, the same as its optical D_{25} diameter. Their position-velocity map indicates that the Nançay beam with its 3.′6 E-W HPBW does not cover all of the H I emission of this edge-on E-W oriented spiral. In fact, our line flux value of 26.4 Jy km s^{-1} is significantly lower than the 36.3 Jy km s^{-1} measured at Westerbork, while the latter is in agreement with ∼40 Jy km s^{-1} measured at Green Bank and Jodrell Bank, whose beams should cover the entire H I disk.

NGC 5533: short Westerbork H I synthesis observations (Broeils & van Woerden 1994) show that its radial H I distribution is symmetric and that it extends out to 2.4 times the optical D_{25} diameter of the galaxy (3.′2), measured at a surface density level of 1 $M_\odot$ pc^{-2}. The integrated line flux measured at Westerbork (35.3 Jy km s^{-1}) is much larger than the Nançay and Green Bank single dish fluxes (19 and 12 Jy km s^{-1}, respectively), and the Arecibo flux (8 Jy km s^{-1}) is even smaller. The linewidths of the Westerbork and single-dish profiles are comparable, however. The discrepancy between the Westerbork and Green Bank line fluxes is puzzling, as the Green Bank 10.′7 HPBW should cover the bulk of the H I emission, seen the 7.′7 H I disk major axis measured at Westerbork.

NGC 5544/5: Very close interacting pair, the nuclei are separated by only 0.′6. Our Nançay values are in agreement with the 7 published Arecibo, Effelsberg and Green Bank profiles, while the Nançay values of Bottinelli et al. (1982) show a considerably higher line flux and linewidths.

NGC 5557: not detected in our survey (estimated $I_{\rm HI} < 2.6$ Jy km s^{-1}). Classified as an elliptical; the upper limit to its gas content ($M_{\rm HI}/L_B < 0.02\ M_\odot/L_{\odot,B}$) is consistent with its classification.

NGC 5589: Though our H I velocity and linewidths are comparable to the Arecibo values listed in the Huchtmeier & Richter (1989) catalogue, our integrated line flux of 1.5 Jy km s^{-1} is considerable higher than the uncertain 0.53 ± 0.36 Jy km s^{-1} listed as the Arecibo value. However, this Arecibo reference, referred to as "Richter & Williams 1989, to be submitted" in the Huchtmeier & Richter catalogue, has apparently never appeared in print.

Table 5. Nançay H I line data for the control group sample.

GH	Ident.	RA	Dec.	$V_{\rm HI}$	$I_{\rm HI}$	W_{50}	W_{20}	rms	$M_{\rm HI}$ [log]	L_B [log]	$M_{\rm HI}/L_B$
No.	No.	(2000.0)		km s^{-1}	Jy km s^{-1}	km s^{-1}	km s^{-1}	mJy	$M_\odot$	$L_{\odot,B}$	$M_\odot/L_{\odot,B}$
(1)	(2)		(3)	(4)	(5)	(6)	(7)	(8)	(9)	(10)	(11)
49	N2998	09 48 44	44 04 52	4778 ± 5	17.5	371	465	3.6	10.24	10.58	0.46
	N3009	09 50 11	44 17 40	—	<2.4	—	—	2.7	<9.38	10.48	<0.08
	U5295	09 52 54	42 50 55	4787 ± 2	16.8	279	303	3.1	10.23	10.12	1.28
57	N3156	10 12 41	03 07 50	—	<2.6	—	—	2.9	<8.24	9.40	<0.07
	N3165	10 13 31	03 22 32	1329 ± 7	5.9	153	225	2.9	8.58	8.84	0.55
	N3166	10 13 45	03 25 31	1356 ± 8	12.0	66	218	5.9	8.89	10.14	0.06
	N3169	10 14 14	03 28 08	1238 ± 4	59.2	363	479	5.8	9.58	10.22	0.23
89	U6617	11 39 17	09 57 22	—	<2.0	—	—	2.3	<9.50	10.30	<0.16
	N3817	11 41 53	10 18 07	6106:	2.1	270:		2.9	9.61	10.31	0.16
	N3822/5*	11 42 18	10 16 16	—	<2.5	—	—	2.7	<9.58	10.71	<0.08
	I724	11 43 35	08 56 31	5966 ± 6	2.6	497	508	2.3	9.61	10.62	0.10
	N3839	11 43 54	10 46 59	5903 ± 13	8.7	301	338	3.8	10.21	10.57	0.44
	N3843	11 43 54	07 55 32	—	<2.1	—	—	2.4	<9.53	10.41	<0.13
118	N5141	13 24 52	36 22 40	—	<2.3	—	—	2.5	<9.46	10.41	<0.11
	N5142	13 25 01	36 23 58	—	<2.2	—	—	2.4	<9.97	10.25	<0.16
	N5149	13 26 10	35 56 04	5652 ± 7	4.7	381	407	3.1	9.78	10.37	0.26
123	N5289	13 45 09	41 30 09	2526 ± 4	9.4	357	379	3.8	9.42	9.69	0.54
	N5290	13 45 19	41 42 55	2573 ± 6	11.7	461	477	4.5	9.52	9.95	0.37
	N5297	13 46 24	43 52 25	2409 ± 2	43.7	391	418	5.9	10.09	10.31	0.60
	N5311	13 48 56	39 59 07	—	<2.4	—	—	2.6	<8.83	9.83	<0.10
	U8736	13 49 04	39 29 56	2384 ± 13	2.8	245	286	3.5	8.90	9.57	0.21
	N5313	13 49 45	39 59 10	2562 ± 29	6.9	409	520	6.9	9.29	10.19	0.13
	N5320	13 50 21	41 22 06	2619 ± 2	19.5	297	315	4.8	9.74	10.09	0.45
	N5326	13 50 51	39 34 29	2513 ± 36	1.0	387	469	2.5	8.45	10.11	0.02
	N5336	13 52 11	43 14 34	2336 ± 4	7.7	186	227	3.0	9.34	9.84	0.25
	N5337	13 52 23	39 41 15	2165 ± 17	2.9	397	435	3.5	8.91	9.93	0.10
	N5350/4*	13 53 24	40 20 00	2321 ± 3	23.9	292	316	6.9	9.83	10.65	0.15
	N5353	13 53 27	40 17 03	2325 ± 3	18.3	291	311	5.0	9.71	10.48	0.17
	N5355	13 53 46	40 20 17	2342 ± 24	2.6	259	315:	5.7	8.86	9.68	0.15
	N5362	13 54 54	41 18 51	2178 ± 4	7.9	258	275	3.8	9.35	9.99	0.23
	N5371	13 55 41	40 27 44	2558 ± 3	24.4	391	409	5.5	9.84	10.72	0.13
	N5383	13 57 05	41 50 44	2270 ± 3	18.0	292	328	4.2	9.70	10.43	0.19
155	N5934	15 28 12	42 55 49	5701 ± 23	3.5	131	382	2.8	9.72	10.15	0.37
	N5945	15 29 45	42 55 14	5523 ± 6	4.3	348	362	2.3	9.80	10.47	0.13
	I4562	15 35 58	43 29 40	—	<1.7	—	—	1.8	<9.39	10.46	<0.08
	I4564	15 36 27	43 31 08	5981 ± 14	3.8	433	516	2.4	9.75	10.22	0.34
	I4566	15 36 43	43 32 24	5774 ± 15	1.6	236	275	2.3	9.38	10.34	0.11
	I4567	15 37 13	43 17 54	5738 ± 6	6.5	300	337	2.3	9.98	10.58	0.25

Note: $I_{\rm HI}$: upper limits are 3σ for 300 km s^{-1} wide, flat-topped profiles; ":" denotes an uncertain value.

No confusion is expected at Nançay from the S0 galaxy NGC 5590 (see below), which lies at an E-W separation of 2.′8 from NGC 5589.

NGC 5590: not detected in our survey (estimated $I_{\rm HI} < 2.8$ Jy km s^{-1}). Classified as a lenticular; the upper limit to its gas content ($M_{\rm HI}/L_B < 0.10\ M_\odot/L_{\odot,B}$) is consistent with its classification.

NGC 5614 (= Arp 178): Four of the 5 published H I velocities agree, except for the ∼43 km s^{-1} higher Green Bank value by Richter & Huchtmeier (1991). Our W_{50} linewidth of 138 km s^{-1} is comparable to the Arecibo value listed in Huchtmeier & Richter (1989) but much smaller than the Green Bank and Nançay literature values of 220–250 km s^{-1}, though our W_{50} value of 246 km s^{-1} is comparable to the published values.

NGC 5656: our Nançay values agree with the published Nançay values (Theureau et al. 1998), if we multiply their integrated line flux (6.1 Jy km s^{-1}) by a factor of 1.26 to convert their flux calibration to the one we adopted (see Matthews et al. 2000, and references therein) and with the Arecibo measurement of 7.9 Jy km s^{-1} listed in Huchtmeier & Richter (1989); surprisingly, the galaxy was not detected ($I_{\rm HI} \leq 3.0$ Jy km s^{-1}) at Arecibo by Krumm & Salpeter (1980).

NGC 5675: this SBb spiral with a LINER spectrum was not detected in our Nançay survey (estimated

$I_{\rm HI} < 2.2$ Jy km s^{-1}), nor at Arecibo (see Table 7). The best upper limit on its $M_{\rm HI}/L_B$ ratio, 0.10 $M_\odot/L_{\odot,B}$, is quite low for its type.

NGC 5695: this SBb with a Seyfert2 spectrum was not clearly detected in our Nançay survey (estimated $I_{\rm HI} < 2.4$ Jy km s^{-1}), which is consistent with Arecibo detections. The upper limit on its $M_{\rm HI}/L_B$ ratio, 0.10 $M_\odot/L_{\odot,B}$, is low for its classification.

Group GH 153:

NGC 5929/30 (= Arp 90): very close pair (0.′5 separation), well within the Nançay beam and clearly detected. NGC 5929 is a $B_{\rm T}$ 14.1 mag Sab:pec with a Seyfert2 spectrum and NGC 5930 is a $B_{\rm T}$ 13.5 mag SABbpec, and their difference in optical radial velocity is 150 km s^{-1}. H I line absorption was detected towards the nuclear region of NGC 5929 with MERLIN (Cole et al. 1998).

UGC 9858: our integrated line flux (30 Jy km s^{-1}) is lower than the 40–50 Jy km s^{-1} measured at Green Bank. This may well be due to missed flux at Nançay, as the E-W D_{25} diameter of the galaxy is about 4.′2, somewhat larger than the E-W HPBW of 3.′6. Our center velocity and linewidth are comparable to the published values, however.

Group GH 156:

A grid of pointings with 5′ spacing in this group was mapped at Arecibo (Zwaan 2000, 2000) as part of a targeted search for H I clouds in galaxy groups. No such clouds were detected at an rms noise level of ∼0.75 mJy for a 10 km s^{-1} resolution, implying a 5σ upper limit of about 6.5×10^6 $M_\odot$ for H I clouds with an H I linewidth of 10 km s^{-1} at the distance we adopted for this group, 27.2 Mpc.

NGC 5951: short Westerbork H I synthesis observations (Rhee & van Albada 1996) show an H I diameter of 3.′4 at a surface density level of 1 $M_\odot$ pc^{-2}, 1.1 times the optical D_{25} diameter. Two integrated line flux measurements of the galaxy are considerable higher than the ∼18 Jy km s^{-1} measured in 5 other studies, for unclear reasons: the 32.5 Jy km s^{-1} measured at Arecibo by Freudling (1995) and the 27.6 Jy km s^{-1} measured at Jodrell Bank by Staveley-Smith & Davies (1988).

NGC 5953/4 pair: was mapped in H I at the VLA (Chengalur et al. 1994). R-band CCD imaging shows that the galaxies are joined by a broad stellar bridge, while NGC 5953 shows an extension towards the north-west. At this position angle an H I plume extends from the galaxy. The overall H I distribution is complex, as is the velocity field, particularly that of NGC 5953 and no clear picture can be drawn of the various kinematical components and their relation to the two galaxies. The total measured H I mass of the system is $1.3{\times}10^9$ $M_\odot$ (equivalent to $F_{\rm HI} = 8.0$ Jy km s^{-1}), of which the authors could readily associate $0.2{\times}10^9$ and $0.5{\times}10^9$ $M_\odot$ with NGC 5953 and 5954, respectively. NGC 5953 is an SAa:pec with a LINER/Seyfert2, and NGC 5954 an SAB(rs)cd:pec with a Seyfert2 spectrum.

In our Nançay profile, two adjacent but distinct peaks can be seen, one with $V = 1700$ km s^{-1}, $I_{\rm HI} = 3.4$ Jy km s^{-1}, $W_{50} = 116$ km s^{-1} and $W_{50} = 133$ km s^{-1}, and the other with $V = 1966$ km s^{-1} and $W_{50} = 146$ km s^{-1}. Nançay and Green Bank profiles centered on the NGC 5953/4 pair will be confused by H I emission from nearby UGC 9902, a $B_{\rm T}$ 17 mag, 0.′9 diameter SBdm? spiral located 3′ due south of the pair. Chengalur et al. (1994) note its VLA detection without giving detailed global profile parameters. At Arecibo, whose small beam should avoid confusion with the NGC 5953/4 pair, Haynes (1981) measured $V = 1695$ km s^{-1}, $W_{50} = 106$ km s^{-1} and an integrated H I line flux of 3.4 Jy km s^{-1} for UGC 9902 (compared to 8.0 for the NGC 5953/4 pair). We therefore conclude that the 1700 km s^{-1} peak in our spectrum is due to nearby UGC 9902.

NGC 5962: Nançay profiles of this galaxy ($V = 1957$ km s^{-1}, $I_{\rm HI} = 16$ Jy km s^{-1}) will be slightly confused by UGC 9925, a $B_{\rm T}$ 15.4 mag Sc spiral 10.′1 due south of it. Arecibo H I profiles of UGC 9925 (Lewis et al. 1985; Sulentic & Arp 1983), which are certainly not confused by NGC 5962 due to the small HPBW, show it has $V = 1916$ km s^{-1}, $FWHM = 182$ km s^{-1} and $I_{\rm HI} = 1.9$ Jy km s^{-1}. One Green Bank observation (Magri 1994) has a much smaller line flux (7.0 Jy km s^{-1}) than the average 16 Jy km s^{-1} found in 7 other studies.

4.1.2. Control group sample

Group GH 49:

NGC 2998: short Westerbork observations (Broeils & van Woerden 1994) show its H I distribution to be symmetric but not very extended compared to its optical dimensions. Full Westerbork H I synthesis mapping (Broeils 1992) show that its H I disk has a diameter of 3.′8 (1.3 D_{25}) and a regular velocity field with a classical, flat rotation curve at $V_{\rm rot} = 210$ km s^{-1}.

Three small spiral companions were detected in H I at Westerbork: NGC 3002, NGC 3006 and MCG 07-20-057. These are $B_{\rm T}$ 15–16 mag objects at distances of 5′ to 12′ from NGC 2998, of about 0.′65 diameter and with integrated H I fluxes ranging from 1.7 to 5.1 Jy km s^{-1} at about the same systemic velocity as NGC 2998 (Broeils 1992). They lie well outside the Nançay HPBW, but can cause some confusion in Green Bank and Jodrell Bank profiles of NGC 2998. Our Nançay profile (estimated $I_{\rm HI} = 17.5$ Jy km s^{-1}) agrees well with that of Theureau et al. (1998). The Green Bank (7.0 Jy km s^{-1}) and Jodrell Bank fluxes (31.9 Jy km s^{-1}) are quite different, though central velocities and linewidths are consistent between all available profiles.

NGC 3009: our narrow "detection" seen in Fig. 1b is in fact spurious and due to radio interference, which occurs in the H polarization only. The upper limit listed in Table 6 was derived from the unaffected V polarization data only. This Sc spiral was reported as detected at Green Bank by Haynes et al. (1988), who noted that their

Table 6. Published H I line data – interacting group sample.

GH	Ident.	V_{HI}	I_{HI}	W_{50}	W_{20}	Tel.	Ref.	Ident.	V_{HI}	I_{HI}	W_{50}	W_{20}	Tel.	Ref.
No.		km s^{-1}	Jy km s^{-1}	km s^{-1}	km s^{-1}				km s^{-1}	Jy km s^{-1}	km s^{-1}	km s^{-1}		
(1)	(2)	(3)	(4)	(5)	(6)	(7)	(8)	(2)	(3)	(4)	(5)	(6)	(7)	(8)
45	N2798*	1740	11.1	339	348	G	PS74	N2798/9	1740	10.9		380	G	PS74
		1744	8.6	236		G	H82	N2799*	1757	9.6			G	DS83
		1778	9.0			G	DS83		1755	11.1	343	385	N	B82
		1726	11.1:	274	345	N	B80		1865	2.0	121		V	N97
		1669	3.2		175	N	vB85	N2844	1486	5.8	310		G	H82
		1747	3.0	277		V	N97		1479	7.0	329		G	M94
58	N3162	1290	21.5	164	237	A	BC79	N3189	1373	6.2		605	A	WR87
		1302	26.6:	176	190	G	DR78		1518	6.8			G	DS83
		1373	6.2		605	A	WR87		1314	4.4		478	N	BC83
		1302	28.6	178	191	J	D80		1320	5.1		528	V	W91
		1302	44.1	183	273	N	B82	N3189/90	1302	4.1		457	A	Ha81
	N3177	1299	6.1	180		A	KS80	N3193		<0.4			V	W91
		1296	3.3		204	A	Ha81	N3213	1347	1.7	160		A	BG87
		1317	5.1	195	301	A	BC79	N3227*		15.2:			A	DS83
		1303	6.4:	230	410	N	B82		1169	6.8:	387:		A	C87
	N3185	1218	6.1	241		A	KS80		1146	12.8:		526:	A	M82
		1234	3.4		278	A	Ha81		1146			526:	A	MW84
		1226	3.7		253	A	WR87		1152	13.3:	407	475	A	B79
		1237	7.3:	266		G	H82		1138	28.6:	364	471	E	HB75
		1239	3.5		253	N	BC83		1165	18.4:	109	374	G	P79
		1200	3.3		308	V	W91		1148	14.1:			G	DS83
	N3187	1577	8.3			A	DS83		1106	20.2:	366:	400:	G	H78
		1580	10.7		245	A	WR87		1199	18.9:	258	300	J	LD73
		1579	10.5	224	276	A	GS85			20.7			V	W95
		1579	9.6		262	A	Ha81	N3239	754	53.0	144		A	He81
		1558	7.5:			G	H82		756	60.9			A	DS83
		1581	12.6			G	DS83		754	88.0	160	205	G	FT81
		1582	10.3	219	243	J	S88		755	80.2:	153	192	G	S78
		1573	24.6:	220	383	N	B82		751	73.2:	157	210	G	DR78
		1591	14.2		261	N	BC83		750	78.8		197	G	TC88
		1541	10.6		277	V	W91		751	73.2			G43	DS83
	N3189	1310	3.2		441	A	LS84		751				G	RD76
67	N3381	1627	21.0	80		A	KS80	U6070	1849	6.2	118		A	BG87
		1631	8.5	56	125	A	L87	N3430	1586	44.1	340		A	HS82
		1630	11.5	117		A	M94		1594	42.1	337	351	G	DR78
	N3395*	1620	20.2	176	225	A	L85		1577	57.1	338	370	J	S88
		1621	16.0		223	A	J87		1583				G	T78
		1631	38.4:	134:	228	G	S75		1594				G	RD76
		1621				G	RD76		1583					F71
		1605				G43	F71	N3442	1729	4.2	120	196	A	T81
		1625				V	C99		1732	3.1	147		A	BG87
	N3396*	1625	26.1	162		A	KS80			3.1	130		A	BG87
		1684				V	C99		1736	2.0		143	A	J87
	N3395/6		26.0			V	C99		1731	9.1	161		A	M94
	N3424	1501	14.0	353		A	HS82							
86	N3786*	2672	12.1			A	DS83	N3786*		confused			A/W	OS93
		2707	9.1		545	A	MW84	N3788*	2687	9.4	501	562	A	L85
		2725	4.9	331	401	A	L85		2712	13.0	391	516	A	S86
		2770	8.1:	288	452	A	S86		2673	11.8	509		A	M94
		2703	9.7	480		A	M94			confused			A/W	OS93
		2718	15.4			G	DS83							
92	N3902	3601	8.8	239	261	A	L85	N3997	4765	8.8		295	A	Wi86
	N3920	3640	6.9	184	218	N	G94		4771	7.0		283	A	GZ87
	U6806	3760	4.2		265	A	Wi86	N4005	4458	2.0		402	A	Wi86
	I746	5027	7.4	271	309	A	L85		4470	2.1		463	A	GZ87
		5030	6.7		310	A	Wi86		4469	1.4	360		A	C93
		5027	7.7		293	A	GZ87	N4015	4368	2.8	522	700	E	H95
	N3987	4501	7.9		557	A	Wi86	N4015A*		<1.3			A	Wi86
		4495	6.6		575	A	GZ87	N4015B*	4347	2.3		815	A	Wi86
		4500			575	A	M93	N4022		<1.8			A	Wi86
	N3987	4502	6.7	543		A	C93							

spectrum is probably confused with NGC 3010, which lies well outside the Nançay beam. Their spectrum shows a broad component between ∼4470 and 4900 km s^{-1} at the 8 mJy level and a narrow (∼120 km s^{-1} *FWHM*) 17 mJy peak at ∼4570 km s^{-1}. As the optical velocities of NGC 3009 and 3010 are 4604 ± 50 and 4401 ± 44 km s^{-1}, respecively (LEDA), the association of the 4570 km s^{-1} peak with NGC 3009 seems plausible; surprisingly, we did not detect this peak with our 2.9 mJy rms noise level.

UGC 5295: Our integrated line flux (16.8 Jy km s^{-1}) is comparable to the Green Bank value of 19.6 Jy km s^{-1} from Haynes et al. (1988) but considerable higher than

Table 6. continued.

GH No.	Ident.	V_{HI} km s^{-1}	I_{HI} Jy km s^{-1}	W_{50} km s^{-1}	W_{20} km s^{-1}	Tel.	Ref.	Ident.	V_{HI} km s^{-1}	I_{HI} Jy km s^{-1}	W_{50} km s^{-1}	W_{20} km s^{-1}	Tel.	Ref.
(1)	(2)	(3)	(4)	(5)	(6)	(7)	(8)	(2)	(3)	(4)	(5)	(6)	(7)	(8)
126	N5341	3648	6.2	246		G	P79	N5394*	3490	32.0:	454		A	KS80
	N5351	3630	18.4	421	458	G	P79		3472	18.4	511	601	N	T98
		3377	23.1	420	445	J	S87	N5395*	3490	32.0:	454		A	KS80
		3605	19.2	445	528	N	B82		3445	16.0		606	A	SA83
		3610	20.2	407	443	W	R96		3544	24.5			G	DS83
		3611				G	T78		3459	28.3	470		G	RH91
	N5378	2947	11.2	440	490	G	RH91		3498	22.9	540	632	J	S87
		2990		325	335	N	T98		3505	17.9:	570:	681:	N	B82
	N5380		<1.3			A	C87		3459	29.9			N	C77
			<6.3			E	H82							
141	N5529	2878	41.3	597	596	G	FT81	N5545*	3079	4.4	298	286	A	F95
		2882	37.7	571	606	G	S78		3051	4.2			G	DS83
		2882	27.1	570	603	A	L85		3088	6.0	350	430	N	B82
		2888	41.0	561	587	J	S88	N5589	3394	0.53	171	186	A	HR89
		2880	41.0	585	630	G	RH91			<5.4			G	RH91
		2895	36.3	557	600	W	R96	N5614	3884	2.3	126	219	A	HR89
	N5533	3867	8.3	451	465	A	Le85		3889	3.7			G	DS83
		3867	8.3	451	465	A	L85		3934	4.2	250	285	G	RH91
		3864				G	T78		3899	5.8:	220		N	B80
		3859	12.0			G	RH91	N5656		<3.0			A	KS80
		3858	35.3	409	439	W	BW94		3156	7.9	359	393	A	HR89
	N5544*	3072	3.3	253	286	A	SK78		3150	6.1	350	366	N	T98
		3086	4.1	239	274	A	L87	N5675		<4.5			A	H83
		3078	2.2		234	E	H97			<3.1			A	HR89
		3090	3.0	220	245	G	RH91	N5695	4225	1.6		376	A	MW84
	N5545*	3084	4.3			A	DS83		4255	2.7	338	364	A	HR89
153	N5929*	2561	3.1	211		E	H82	U9858	2619	50.6	366	381	G	FT81
	N5930*	2498	4.1	325	385	G	RH91		2630	41.0			G	DS83
		2530				N	T98		2622				G	T78
156	N5951	1776	17.9		279	A	Ha81	N5953*	1969	5.4		283	A	M88
		1782	16.0	263	289	A	GS85		1965	7.3	136		A	C93
			32.5	293	292	A	F95		1950	7.0:	158:	235:	N	B82
		1784	20.2	264	227	G	FT81		1921:		280:		V	C94
		1779	19.1		288	G	TC88	N5954*	1935	7.2		275	A	Ha81
		1777	27.6	264	277	J	S88		1938	5.9			A	DS83
		1779	20.2	265	282	W	R96		1960	7.4	146	279	A	L85
	N5962	1955	17.1:	346		A	KS80		1955	7.8	126	235	A	GS85
		1957	15.4	345		A	G87		1971	6.9	125		A	G87
		1958	13.2		364	A	M88		1964	7.2	133		A	C93
		1958	16.7	343		A	C93			13.1	276	275	A	F95
		1963	17.6:	342	354	G	S78		2000	4.1:			G	S78
					362	G	S78		1969	9.1:			N	B82
		1948	7.0	351		G	M94		1903		217		V	C94
		1960	15.0	350	412	N	B82	N5953/4		8.0			V	C94
	N5953*	1964	6.5	140		A	G87							

Note: ":" denotes an uncertain value.

the Nançay value of 11.5 Jy km s^{-1} reported by Bottinelli et al. (1982).

Group GH 57:

NGC 3156/65/66/69: H I in the NGC 3169 group, i.e. the Garcia 192 group (Garcia 1993), was mapped at Arecibo in the NGC 3165/66/69 area by Haynes (1981) and extended towards NGC 3156 by Duprie & Schneider (1996). These observations show complex H I distributions and kinematics: H I is definitely associated with NGC 3166 and NGC 3166, and detected at and near the position of NGC 3165, but the physical association of this emission with this late-type spiral is unclear. No H I is detected in the S0 NGC 3156; the rms noise of Duprie & Schneider, 1.98 mJy, gives an upper limit of 1.8 Jy km s^{-1} to the integrated line flux. The estimated total H I line flux of the group is 128 Jy km s^{-1} from the Arecibo mapping of Haynes et al. (1981) and 105 Jy km s^{-1} from the Nançay mapping by Balkowski & Chamaraux (1983). Clearly, the 3 Nançay pointings (centered on NGC 3165, 3166 and 3169) will not cover the extended H I distribution of the group. The extension of the H I distribution is also evident from the flux densities of spectra taken in the direction of NGC 3166: 39.1 Jy km s^{-1} at Green Bank, 12 at Nançay and 3.5 at Arecibo. Our linewidths for NGC 3166 are much narrower than the 2 literature values, probably due to complex confusion in its vicinity; Haynes (1981) noted a narrow velocity component (presumably associated with the galaxy) superposed on a broad component at and near the galaxy's position. For NGC 3169, compared to our Nançay integrated line flux (59 Jy km s^{-1}), the two published Nançay spectra have either a much larger (99 Jy km s^{-1}) or a much smaller (24 Jy km s^{-1}) flux,

and the latter (Bottinelli et al. 1970) has a much smaller W_{50} width, though its W_{20} width is comparable to ours. NGC 3166 is an SABO$^-$a with a LINER spectrum, and NGC 3169 is an SA(s)apec with a LINER spectrum.

Group GH 89:

UGC 6617: lenticular galaxy, not detected in our survey (estimated $I_{\rm HI} < 2.0$ Jy km s^{-1}). The Arecibo upper limit of 1.5 Jy km s^{-1} listed in Table 7, from Williams (1985), has been corrected to the line width of 300 km s^{-1} used for upper limits throughout the present paper. We assume this to be a 3σ upper limit, though this is not mentioned explicitly in Williams' paper.

NGC 3817: our integrated line flux of 2.1 Jy km s^{-1} is much higher than the Arecibo value of 1.1 ± 0.23 Jy km s^{-1} reported by Williams (1985), but our detection has a peak flux density of 3.5σ only and our line flux is therefore not very accurate.

NGC 3822/5: pair of spirals not clearly detected in our survey (estimated $I_{\rm HI} < 2.4$ Jy km s^{-1}). The pair is oriented practically East-West, with a separation of 3.′1, somewhat smaller than the Nançay E-W HPBW and the Arecibo HPBW. Our non-detection is surprising, given the integrated Arecibo line fluxes of 3.6 and 0.8–1.6 Jy km s^{-1} reported for NGC 3822 and 3825, respectively, by Eder et al. (1991) and Williams (1985). This may indicated the presence of extended H I emission outside the Nançay beam area. NGC 3822 has a Seyfert2 spectrum.

IC 724: our integrated line flux (2.6 Jy km s^{-1}) is lower than the 3.5–4.8 Jy km s^{-1} measured at Arecibo, and our W_{50} value (497 km s^{-1}) is somewhat smaller than the ∼540 km s^{-1} measured at Arecibo.

NGC 3843: S0/a galaxy, not detected in our survey (estimated $I_{\rm HI} < 2.1$ Jy km s^{-1}). The upper limit to its H I gas content, $M_{\rm HI}/L_B < 0.13\ M_\odot/L_{\odot,B}$, is consistent with its morphological classification.

Group GH 118:

NGC 5141 and NGC 5142: two S0 galaxies, not detected in our survey (estimated $I_{\rm HI} < 2.3$ and <2.2 Jy km s^{-1}, and $M_{\rm HI}/L_B < 0.11$ and $<0.16\ M_\odot/L_{\odot,B}$, respectively).

NGC 5149: Detected at Nançay by Theureau et al. (1998) and in the present survey (at $I_{\rm HI}$ 4.7, 6.6 Jy km s^{-1}, respectively). Oosterloo & Shostak (1993) did not detect it at Arecibo, but the H I line is too weak for a clear detection at their rms level of 6.6 mJy; in their short Westerbork observations of the NGC 5149/5154 (= UGC 8444/54) pair the signal of NGC 5149 is confused with that of its companion. No confusion with NGC 5154 is expected for the Nançay spectra, since it has an E-W separation of 3.′8 from NGC 5149.

Group GH 123:

NGC 5289/90 pair: mapped in H I at Westerbork (van Moorsel 1983). The H I distribution of NGC 5289 is clearly asymmetric, with an extension towards the NW away from the plane, possibly due to interaction with NGC 5290, which itself does not seem to be affected. The H I kinematics does not indicate that the interaction was important, as reliable classical flat H I rotation curves could be derived from the velocity fields: $V_{\rm rot,max}$ is ∼180 and 225 km s^{-1} for, respectively, NGC 5289 and NGC 5290. The E-W H I diameters of NGC 5289 and 5290 measured at Westerbork are 3.′9 and 37, respectively. The 3.′6 Nançay E-W HPBW should therefore cover the entire H I emission of each object, as shown by the agreement between our profile parameters and the literature values.

NGC 5311: S0/a galaxy, at $V_{\rm opt} = 2698 \pm 40$ km s^{-1}, not detected in our survey (estimated $I_{\rm HI} <$ 2.4 Jy km s^{-1}). Detected at Green Bank (Richter & Huchtmeier 1991), with a considerably higher integrated line flux, 5.1 Jy km s^{-1}, at $V = 2645$ km s^{-1}, with $W_{50} = 453$ km s^{-1}. The Green Bank profile could in principle be confused with NGC 5313, a $B_{\rm T}$ 12.8 mag, Sbc type spiral 9.′3 due East of NGC 5311, with $V_{\rm opt} = 2597 \pm 44$ km s^{-1}. Three H I detections of NGC 5313 are available: one from Green Bank (Peterson 1979) and two from Nançay (Bottinelli et al. 1982; the present survey); in principle, the Nançay detections should not be confused by emission from NGC 5311. The H I profile parameters of NGC 5313 are $V = 2551$ km s^{-1}, $I_{\rm HI} = 9.5$ Jy km s^{-1} and $W_{50} = 421$ km s^{-1}. Because the separation between the two galaxies is comparable to the size of the Green Bank beam, the "detection" of NGC 5311 could be due to the higher velocities in the NGC 5313 profile.

NGC 5320: of the 4 the available Green Bank, Jodrell Bank and Nançay profiles, the Green Bank profile of Magri (1994) is discrepant, having ∼3.5 times smaller integrated line flux (7 Jy km s^{-1}), though its central velocity and linewidths are comparable to those of the others.

NGC 5326/5337: short Westerbork H I synthesis observations were made of this pair (Oosterloo & Shostak 1993), but the galaxies were not detected at an rms noise level of 3.0 mJy/beam (resolution 25″).

NGC 5336 our integrated line flux (7.7 Jy km s^{-1}) is higher than the 5.4 Jy km s^{-1} measured at Nançay by Theureau et al. (1998). This general tendency, due to differences in calibration procedures, has already been discussed in Matthews et al. (2000), and references therein.

NGC 5350/3/4/5 area: 5 galaxies constitute Hickson Compact Group 68: NGC 5350, 5353, 5354, 5355 and 5358 (Hickson 1982). NGC 5350/3/4: three closeby galaxies are located near the centre of the Nançay beam in the pointings towards NGC 5350/4 and NGC 5353: the SBb spiral NGC 5350 ($V_{\rm opt} = 2321 \pm 61$ km s^{-1}) and the early-type (E/S0) systems NGC 5353 ($V_{\rm opt} = 2166 \pm 103$ km s^{-1}) and NGC 5354($V_{\rm opt} = 2681 \pm 244$ km s^{-1}). In principle, Arecibo or radio synthesis observations could separate the H I emission from the galaxies, but no Arecibo data are available (see Table 7), and no mention was made of the detection of H I in either NGC 5353 or NGC 5354 in the short Westerbork observations of NGC 5350 (Rhee & van Albada 1996). As we do not expect the two early-types to be detectable in H I, and as our two Nançay

Table 7. Published H I line data – control group sample.

GH No.	Ident.	V_{HI} km s^{-1}	I_{HI} Jy km s^{-1}	W_{50} km s^{-1}	W_{20} km s^{-1}	Tel.	Ref.	Ident.	V_{HI} km s^{-1}	I_{HI} Jy km s^{-1}	W_{50} km s^{-1}	W_{20} km s^{-1}	Tel.	Ref.
(1)	(2)	(3)	(4)	(5)	(6)	(7)	(8)	(2)	(3)	(4)	(5)	(6)	(7)	(8)
49	N2998	4766	7.0	386		G	M94	N2998	4790	20.1	382	394	W	BW94
		4777				G	T78		4781	21.4	394	417	W	B92
		4700				G	FT81	N3009	4666	3.7	103	443	G	H88
		4777	31.9	374	392	J	S88	U5295	4790	19.6	286		G	H88
		4784	14.7	373	389	N	T98		4771	11.5	261	332	N	B82
57	N3156		1.4	690		A	K79	N3166	1283	3.5		435	A	Ha81
			<1.8			A	DS96		1418	4.6			A	DS83
			<1.0			A	K78		1328	39.1:	177		G	H82
			<0.7			A	G83	N3166/9	1239	105.0		443	N	BC83
	N3165	1335	3.3		150	A	Ha81	N3169	1234	42.5			A	DS83
		1328	3.9	139	156	A	L85		1227	58.1		481	A	Ha81
		1332	4.9		141	N	BC83		1240	96.0	537		G	DS83
		1340	2.9	157	173	A	S90		1229	25.0::	195:	505:	N	B70
		1356	7.9	159	—	A	DS96		1240	98.9			N	B79
89	U6617		<1.5			A	W85	N3825*	6323	0.8		393	A	W85
	N3817	6079	1.1		326	A	W85	I724	5972	3.5		551	A	W85
	N3822*	6164	3.6	545	552	A	E91		5963	4.2	543	545	A	E91
		6168	4.2	521		A	M94		5973	4.8	538		A	M94
		6166	3.6		559	A	W85	N3839	5910	10.1		366	A	W85
	N3825*	6381	1.6	611	608	A	E91							
118	N5141		<7.2			A	DS83	N5149	5660	6.6	453	462	N	T98
	N5142		<6.0			A	OS93	N5149/55	confused				A/W	OS93
123	N5289	2516	8.8	371		G	P79	N5337	not detected				W	OS93
		2525	7.3	360	374	W	V83	N5350*	2198	23.1	265	435	N	B82
		2521	9.0		401	G	TC88		2316	30.5	282	298	G	FT81
		2493	9.7		380	N	Pun		2322	29.9	292	316	J	S87
	N5290	2579	12.1:	469	484	G	FT81		2321	30.2	295	332	W	RA96
		2583	10.4	461		G	P79	N5354*	2304	19.1	266	301	E	RH91
		2571	11.1	453	475	W	V83	N5353	2307	17.7	300	308	E	RH91
		2589	11.7	444	473	J	S87		2310	17.1	300	388	E	H94
		2572	10.6		482	G	TC88			<10.7			G	DS83
	N5297	2406		417	480	N	B82	N5355	2313	14.7	289	305	E	RH91
		2392	52.0:	402	423	J	D80		2340	17.5	290	336	G	WR86
		2404	52.0	394	427	G	FT81	N5362	2166	8.2	258	272	E	RH91
		2411	52.0			G	DS83		2169	7.0	274		G	M94
		2405	54.0			G43	DS83		2182	7.1	264	280	N	T98
	N5311	2645	5.1	390	425	G	RH91		2175	9.5	296		W	K96
	U8736		<8.1			G	RH91	N5371	2557	40.2:	384	420	G	S78
	N5313	2540	12.1	448	478	N	B82		2555	33.4:	377	399	J	D80
		2537	8.4	421		G	P79		2541	29.1	400	475	N	B82
	N5320	2613	25.4	300	313	G	FT81		2554	26.6	382	411	W	We86
		2619	28.6	300	313	J	SD88			30.1			W	B87
		2609	7.0	314		G	M94	N5383	2264	15.3:	306:	339:	G	P78
	N5326		<2.7			G	RH91		2268				G	T78
			not detected			W	OS93		2165	27.0:	309	346	G	TM81
		2520	1.8	335	337	N	T98		2265	28.1	290	327	J	SD87
	N5336	2324	7.0	218		G	M94		2282	36.0	382	497	N	B82
		2338	5.4	211	216	N	T98		2264	22.0	303	327	W	A74
	N5337	2125	1.8	344	355	G	GH91		2264	22.1	315	340	W	S79
		2102	3.3	370	429	N	T98							
155	N5945	5516	3.7	356	456	N	T98	I4567	5722				G	T78
			<5.4			G	RH 91		5795	15.5	380	430	G	RH91
	I4564*	5961	7.5	494	624	A	GH91		5711	7.0	330		G	M94
	I4566*		<4.5			G	RH 91		5737	6.0	320	337	N	T98
		5767	1.5	289	326	N	T98							

Note: ":" denotes an uncertain value.

profiles have very similar profile parameters, we will assume that all gas detected in our Nançay profiles actually resides in NGC 5350. The Rhee & van Albada Westerbork data show an H I diameter of 4′.4 at a surface density level of 1 $M_\odot$ pc^{-2}, 1.1 times the optical D_{25} diameter. NGC 5355: we detected H I in the Nançay spectrum taken towards NGC 5355, an early-type galaxy (classified as S0 or E). Gas-rich S0 galaxies, though rare, do exist (e.g., Wardle & Knapp 1985), and often with large H I distributions (van Driel & van Woerden 1991), but our NGC 5355 H I profile closely resembles the high-velocity half of our strong detection of the large spiral NGC 5350, located 4′.5 W of NGC 5355, though with a six times reduced flux density. We therefore consider this "detection" to be of nearby NGC 5350. In principle, our NGC 5355 Nançay spectrum might be confused with B_T 14.6 mag, S0/a NGC 5358, located 3′.0 E of it, but the only H I "detection" of this object (Richter & Huchtmeier 1991) seems spurious, as its central velocity of 1547 km s^{-1} is completely discrepant with the optical velocities of all nearby galaxies,

including that of NGC 5358 itself (2432±60 km s^{-1}, based on 2 published measurements).

NGC 5362: short Westerbork H I synthesis observations (Kamphuis et al. 1996) were obtained of this object to determine global H I profile parameters (see Table 7); no further morphological or kinematical H I data are given.

NGC 5371: this SAB(rs)bc with a LINER spectrum, was mapped in H I at Westerbork (Wevers et al. 1986). Its optical luminosity profile shows a sharp edge at a radius of about 100″, beyond which the surface brightness drops rapidly and the disk becomes redder. Its H I distribution is ring-shaped with a maximum surface density of 80″ radius, and having an outer edge coinciding with the optical edge. Its velocity field shows signs of a mild warp, and a flat rotation curve was derived from it with a $V_{\rm rot,max}$ of 300 km s^{-1}.

NGC 5383: this barred SBb system was mapped in H I at Westerbork (Sancisi et al. 1979). The atomic hydrogen is largely concentrated in the optically bright central parts, and deficient in the region of the bar. Its kinematics are regular, with deviations of order 50–100 km s^{-1} near the bar (similar to those found in other barred galaxies). A classical flat rotation curve was derived from the velocity field with $V_{\rm rot,max} = 210$ km s^{-1}.

At Westerbork, H I emission was also detected from the SBdm companion UGC 8877, located 3′ South of NGC 5383. The published single-dish H I data for NGC 5383, as well as our data, will be only slightly confused by its presence, as its integrated H I flux is 1.7 Jy km s^{-1}, i.e. 8% of the integrated H I flux of NGC 5383 as measured at Westerbork. Its central velocity, 2370 km s^{-1}, is 120 km s^{-1} higher than that of NGC 5383. The integrated H I line flux we measured for NGC 5383 (18.0 Jy km s^{-1}) is comparable to the Westerbork value of 22.0 Jy km s^{-1}, though it is twice as small as the previously published Nançay value (Bottinelli et al. 1982).

Group GH 155:

NGC 5934: our Nançay profile, with $V_{\rm HI}$ = 5731 km s^{-1} and $W_{50} = 131$ km s^{-1}, centered on this $B_{\rm T}$ 14.6 mag Sb spiral which has a $V_{\rm opt} = 5603 \pm 33$ km s^{-1}, could in principle be confused with that of two galaxies of about similar magnitude and optical diameter: NGC 5935, a nearby (1.′1 separation) $B_{\rm T}$ 15.1 mag Sb spiral having an optical redshift of 5373±60 km s^{-1} (Falco et al. 1999), and PGC 55173 (CGCG 222-012), a $B_{\rm T}$ 15.5 mag Sb spiral at 4.′7 due north having no published optical redshift. No published H I data are available for either of these objects. The close NGC 5934/5 pair actually shows signs of interaction on the blue POSS image, as the outer regions of NGC 5934 are turned towards NGC 5935, which appears to have a faint, stubby tail pointing away from NGC 5934. VLA continuum observations at 2 and 6 cm wavelength (Batuski et al. 1992) detected NGC 5934 only; these authors classified it as an elliptical(?). No optical emission lines were found in NGC 5934 (Sanduleak & Pesch 1987).

IC 4567: of the 5 available Nançay and Green Bank data, only the Green Bank profile of Richter & Huchtmeier (1991) is discrepant, with a ∼70 km s^{-1} higher central velocity, considerable larger widths and 2.4 times larger integrated line flux (15.5 Jy km s^{-1}); radio interference may well be the cause of this. There are no galaxies in the vicinity to cause confusion in the H I observations.

IC 4562: elliptical galaxy, not detected in our survey (estimated $I_{\rm HI} < 1.08$ Jy km s^{-1} and $M_{\rm HI}/L_B < 0.08\ M_\odot/L_{\odot,B}$).

IC 4564/66: first, a single spectrum was obtained pointed towards the mean position of the galaxies' centers. Given the relatively large E-W separation of the galaxies in α (2.′8) compared to the E-W HPBW of 3.′6, spectra were also obtained individually for the center position of each object. These data were used for Table 6.

IC 4567: of the 5 available Nançay and Green Bank data, only the Green Bank profile of Richter & Huchtmeier (1991) is discrepant, with a ∼70 km s^{-1} higher central velocity, considerable larger widths and 2.4 times larger integrated line flux (15.5 Jy km s^{-1}). Radio interference may well be the cause of this. There are no galaxies in the vicinity to cause confusion in the H I observations.

4.2. Integrated H I line fluxes

Aside from calibration errors, uncertainties in the integrated line flux measurements include contributions from systematic measurement errors, baseline subtraction uncertainties, the effects of a finite telescope beam, as well as external errors and various degrees of confusion with emission from nearby galaxies. In Fig. 2 we compare our new raw, integrated Nançay H I fluxes with those from other sources (see Tables 6 and 7). Panels *a*, *b* and *c* show our new fluxes versus, respectively, previous Arecibo, Green Bank 90-m and Nançay measurements, while (for comparison) panel *d* shows a comparison between Green Bank and Arecibo measurements. This provides us with an internal comparison, using the same telescope, as well as an external comparison with other instruments.

All cases where we measured a Nançay flux more than twice as large or more than twice as small as a flux reported in the literature are discussed in Sect. 4.1. These discrepancies are usually related to the presence of extended H I structures in the groups. In a few cases, a single Green Bank measurement differs significantly from other measurements made with the same telescope, which are consistent with our Nançay value. In one case only there is no clear explanation for the discrepancies between line fluxes: NGC 5533, where the Green Bank and Nançay values are much lower than the Westerbork measurement, though the Green Bank beam should have covered the H I disk.

The cases in which large differences were found between line fluxes measured by us and those reported in the literature are: (1) the Nançay-Green Bank comparison shows 5 galaxies or close galaxy pairs with an integrated Green Bank line flux at least twice as large as our Nançay value (in order of increasing Green Bank flux: NGC 3185, 5378, 3166, 3395 and 3239), and 3 galaxies with a Green

Table 8. References and telescope codes to Tables 6 and 7.

A74	Allen et al. (1974)	B79	Balkowski (1979)	BC83	Balkowski & Chamaraux (1983)
B87	Begeman (1987)	BG87	Bicay & Giovanelli (1987)	BC79	Biermann et al. (1979)
B70	Bottinelli et al. (1970)	B80	Bottinelli et al. (1980)	B82	Bottinelli et al. (1982)
B92	Broeils (1992)	BW94	Broeils & van Woerden (1994)	C77	Chamaraux (1977)
C87	Chamaraux et al. (1987)	C93	Chengalur et al. (1993)	C94	Chengalur et al. (1994)
C99	Clemens et al. (1999)	D80	Davies (1980)	DS83	Davis & Seaquist (1983)
DR78	Dickel & Rood (1978)	DS96	Duprie & Schneider (1996)	E91	Eder et al. (1991)
FT81	Fisher & Tully (1981)	F71	Ford et al. (1971)	F95	Freudling (1995)
G87	Garwood et al. (1987)	G94	Garcia et al. (1994)	GZ87	Gavazzi (1987)
G83	Giovanardi et al. (1983)	GS85	Giovanardi & Salpeter (1985)	Ha81	Haynes (1981)
H88	Haynes et al. (1988)	H78	Heckman et al. (1978)	H83	Heckman et al. (1983)
H94	Huchtmeier (1994)	H97	Huchtmeier (1997)	HR89	see Huchtmeier & Richter (1989)
He81	Helou et al. (1981)	HS82	Helou et al. (1982)	H82	Huchtmeier (1982)
H95	Huchtmeier et al. (1995)	HB75	Huchtmeier & Bohnenstengel (1975)	J87	Jackson et al. (1987)
K78	Knapp et al. (1978)	K79	Knapp et al. (1979)	K96	Kamphuis et al. (1996)
KS80	Krumm & Salpeter (1980)	LS84	Lake & Schommer (1984)	Le85	Lewis (1985)
L85	Lewis et al. (1985)	L87	Lewis (1987)	LD73	Lewis & Davies (1973)
M94	Magri (1994)	M82	Mirabel (1982)	MW84	Mirabel & Wilson (1984)
M88	Mirabel & Sanders (1988)	M93	Mould et al. (1993)	N97	Nordgren et al. (1997)
OS93	Oosterloo & Shostak (1993)	PS74	Peterson & Shostak (1974)	P78	Peterson et al. (1978)
P79	Peterson (1979)	Pun	Paturel (1998)	R96	Rhee & van Albada (1996)
RH91	Richter & Huchtmeier (1991)	RD76	Rood & Dickel (1976)	S79	Sancisi et al. (1979)
S86	Schneider et al. (1986a)	S90	Schneider et al. (1990)	S75	Shostak (1975)
S78	Shostak (1978)	SK78	Silverglate & Krumm (1978)	S87	Staveley-Smith & Davies (1987)
S88	Staveley-Smith & Davies (1988)	SA83	Sulentic & Arp (1983)	T78	Thonnard et al. (1978)
T81	Thuan & Martin (1981)	T98	Theureau et al. (1998)	TC88	Tifft & Cocke (1988)
vB85	van der Burg (1985)	V83	van Moorsel (1983)	W85	Williams (1985)
We86	Wevers et al. (1986)	Wi86	Williams (1986)	WR87	Williams & Rood (1987)
W91	Williams et al. (1991)				
A	Arecibo 305 m	E	Effelsberg 100 m	G	Green Bank 91 m
G43	Green Bank 43 m	J	Joddrell Bank 64 m	N	Nançay 94 m equiv
V	VLA	W	Westerbork		

Bank flux at least twice as small as our Nançay value (IC 4567, NGC 2998 and 5320); (2) the Nançay-Arecibo comparison shows one object with an Arecibo flux more than twice as large as the Nançay value (NGC 3442) and 5 objects with an Arecibo flux less than twice the Nançay value (in order of increasing Arecibo flux: NGC 3166, 3786, 3227, UGC 6806 and NGC 5533); (3) a comparison between our Nançay data and profiles obtained earlier with the same telescope shows 2 objects with a literature Nançay flux more than twice as large as our value (in order of increasing flux: NGC 3187 and 5383) and one with a literature Nançay flux less than twice our value: GC 3169.

4.3. H I profile linewidths

In Figs. 3 and 4 we compare, respectively, our directly measured W_{50} and W_{20} linewidths with values from other sources (see Tables 6 and 7). Panels *a*, *b* and *c* show our linewidths versus, respectively, previous Arecibo, Green Bank 90-m and Nançay measurements. Cases where we measured an H I linewidth more than twice as wide or more than twice as narrow as a published linewidth are discussed in Sect. 4.1; these discrepancies are all related to the presence of extended H I structures in the groups.

The cases in which large differences between measured linewidths were found are: (1.) The Nançay-Green Bank comparison shows 2 galaxies or close galaxy pairs with a Green Bank W_{50} measurement more than twice as large as the Nançay value: NGC 3166 and 3226/7 (in order of increasing linewidth); (2) the Nançay-Arecibo comparison shows one object with an Arecibo W_{50} measurement more than twice as large as the Nançay value (NGC 3226/7) and one with a W_{20} more than twice as large as the Nançay value: NGC 3166.

5. Summary and conclusions

The Nançay observations presented in this paper have provided H I line profiles and values or limits on gas masses and H I mass-to-light ratios for 91 members of loose groups. Five of the 11 galaxies in the sample which had not been observed previously, were detected by us (NGC 2852, NGC 5596, NGC 5934, UGC 6070 and UGC 6545) as well as 4 of the 10 galaxies which had not been detected previously (NGC 3193, NGC 5326, NGC 5380 and UGC 8736).

For galaxies which had been previously observed in the H I line, we generally find good agreement in radial velocities, while a larger scatter is seen for the H I line width parameters, especially W_{20}. The line widths are sensitive to the degree of resolution of the target galaxies, especially for the relatively small Arecibo beam, to the presence of tidal debris within the beams and to the quality of the data, in particular for W_{20}. The largest scatter is found in integrated H I fluxes, where differences of ∼50% are common between various observations obtained with the Green Bank 90-m, Arecibo 305-m and Nançay telescopes. Our knowledge of the H I content of even the giant members of relatively nearby groups of galaxy is rather poor.

In a future paper we will analyze the H I, optical and near-infrared properties of the "interacting" and "control" galaxy groups. We also plan to correlate H I properties with galaxy structural characteristics as determined from optical and near-infrared observations.

Acknowledgements. We would like to thank the referee, Dr. M. S. Roberts, for his comments. The Unité Scientifique Nançay of the Observatoire de Paris is associated as Unité de Service et de Recherche (USR) No. B704 to the French Centre National de Recherche Scientifique (CNRS). Nançay also gratefully acknowledges the financial support of the Département du Cher, the European Community, the FNADT and the Région Centre. This research has made use of the Lyon-Meudon Extragalactic Database (LEDA) supplied by the LEDA team at the CRAL-Observatoire de Lyon (France), as well as of the NASA/IPAC Extragalactic Database (NED) which is operated by the Jet Propulsion Laboratory, California Institute of Technology, under contract with the National Aeronautics and Space Administration. Partial support for this program was provided through NASA grant NAG5-7040 and NSF grant AST 99-73812 to P.M.M. and through NSF grant AST-9875008 to E.M.W.

References

Allen, R. J., Goss, W. M., Sancisi, R., Sullivan, W. T., & van Woerden, H. 1974, in The Formation and Dynamics of Galaxies, IAU Symp. 58, ed. J. R. Shakeshaft (Reidel: Dordrecht), 425
Bahcall, N. A., Harris, D. E., & Rood, H. J. 1984, ApJ, 284, 29
Balkowski, C. 1979, A&A, 78, 190
Balkowski, C., & Chamaraux, P. 1983, A&AS, 51, 331
Batuski, D. J., Hanisch, R. J., & Burns, J. O. 1992, AJ, 103, 1077
Begeman, K. 1987, H I rotation curves of spiral galaxies, Ph.D. Thesis, University of Groningen
Bicay, M. D., & Giovanelli, R. 1987, AJ, 93, 1326
Biermann, P., Clarke, J. N., & Fricke, K. J. 1979, A&A, 75, 7
Biermann, P., & Kronberg, P. P. 1984, in Clusters and Groups of Galaxies, ed. F. Mardirossian, G. Giuricin, & M. Mezzetti (Reidel: Dordrecht), 395
Bottinelli, L., Chamaraux, P., Gouguenheim, L., & Lauqué, R. 1970, A&A, 6, 453
Bottinelli, L., Gouguenheim, L., & Paturel, G. 1980, A&A, 88, 32
Bottinelli, L., Gouguenheim, L., & Paturel, G. 1982, A&A, 113, 61
Broeils, A. H. 1992, Dark and visible matter in spiral galaxies, Ph.D. Thesis, University of Groningen
Broeils, A. H., & van Woerden, H. 1994, A&AS, 107, 129
Chamaraux, P. 1977, A&A, 60, 67
Chamaraux, P., Balkowski, C., & Fontanelli, P. 1987, A&AS, 69, 263
Chamaraux, P., Balkowski, C., & Gérard, E. 1980, A&A, 83, 38
Chengalur, J. N., Salpeter, E. E., & Terzian, Y. 1993, ApJ, 419, 30
Chengalur, J. N., Salpeter, E. E., & Terzian, Y. 1994, AJ, 107, 1984
Clemens, M. S., Baxter, K. M., Alexander, P., & Green, D. A. 1999, MNRAS, 308, 364
Cole, G. H. J., Pedlar, A., Mundell, C. G., Gallimore, J. F., & Holloway, A. J. 1998, MNRAS, 301, 782
Corsini, E. M., Pizzella, A., Funes, J. G., Vega Beltran, J. C., & Bertola, F. 1998, A&A, 337, 80
Davies, R. D. 1980, private communication
Davis, D. S., Mulchaey, J. S., & Muchotzsky, R. F. 1999, ApJ, 511, 34
Davis, L. E., & Seaquist, E. R. 1983, ApJS, 53, 269
Dell'Antonio, I., Bothun, G. D., & Geller, M. J. 1996, AJ, 112, 1759
de Vaucouleurs, G., de Vaucouleurs, A., Corwin, et al. 1991, Third Reference Catalogue of Bright Galaxies (New York: Springer) (RC3)
Dickel, J. R., & Rood, H. J. 1978, ApJ, 223, 391
Duprie, K., & Schneider, S. E. 1996, AJ, 112, 937
Eder, J., Giovanelli, R., & Haynes, M. P. 1991, AJ, 102, 572
Falco, E. E., Kurtz, M. J., Geller, M. J., et al. 1999, PASP, 111, 438
Fisher, J. R., & Tully, R. B. 1981, ApJS, 47, 139
Ford Jr., W. K., Rubin, V. C., & Roberts, M. S. 1971, AJ, 76, 22
Fouqué, P., Bottinelli, L., Durand, N., Gouguenheim, L., & Paturel, G. 1990, A&AS, 86, 473
Freudling, W. 1995, A&AS, 112, 429
Fukazawa, Y., Makishima, K., Matsushita, K., et al. 1996, PASJ, 48, 395
Gallagher, J. S., Littleton, F. E., & Matthews, L. D. 1995, AJ, 109, 2003
Garcia, A. M. 1993, A&AS, 100, 47
Garcia, A. M., Bottinelli, L., Garnier, R., Gouguenheim, L., & Paturel, G. 1994, A&AS, 107, 265
Garwood, R. W., Helou, G., & Dickey, J. M. 1987, ApJ, 322, 88
Gavazzi, G. 1987, ApJ, 320, 96
Geller, M. J., & Huchra, J. P. 1983, ApJS, 52, 61
Giovanardi, C., Krumm, N., & Salpeter, E. E. 1983, AJ, 88, 1719
Giovanardi, C., & Salpeter, E. E. 1985, ApJS, 58, 623
Haynes, M. P. 1981, AJ, 86, 1126
Haynes, M. P., Giovanelli, R., & Chincarini, G. L. 1985, ARA&A, 22, 445
Haynes, M. P., Giovanelli, R., Starosta, B. M., & Magri, C. 1988, AJ, 95, 607
Haynes, M. P., Jore, K. P., Barrett, E. A., Broeils, A. H., & Murray, B. M. 2000, AJ, 120, 703
Heckman, T. M., Balick, B., & Breugel, W. J. M. 1983, AJ, 88, 583
Heckman, T. M., Balick, B., & Sullivan III, W. T. 1978, ApJ, 224, 745
Helou, G., Giovanardi, C., Salpeter, E. E., & Krumm, N. 1981, ApJS, 46, 267
Helou, G., Salpeter, E. E., & Terzian, Y. 1982, AJ, 87, 1443
Hernquist, L., Katz, N. S., & Weinberg, D. H. 1995, ApJ, 442, 57
Hickson, P. 1982, ApJ, 255, 382
Hickson, P., Kindl, E., & Weinberg, D. H. 1988, ApJ, 331, 64
Hoffman, G. L., Salpeter, E. E., Lamphier, C., & Roos, T. 1992, ApJ, 388, L5
Huchra, J., Davis, M., Latham, D., & Tonry, J. 1983, ApJS, 52, 89
Huchra, J. P., Geller, M. J., & Corwin, H. G. Jr. 1995, ApJS, 99, 391
Huchtmeier, W. K. 1982, A&A, 110, 121
Huchtmeier, W. K. 1994, A&A, 286, 389
Huchtmeier, W. K. 1997, A&A, 319, 401
Huchtmeier, W. K., & Bohnenstengel, H. D. 1975, A&A, 44, 479

Huchtmeier, W. K., & Richter, O.-G. 1989, A General Catalogue of H I Observations of Galaxies (Springer, Heidelberg)
Huchtmeier, W. K., Sage, L. J., & Henkel, C. 1995, A&A, 300, 675
Jackson, J., Barett, A. H., Amstrong, J. T., & Ho, P. T. P. 1987, AJ, 93, 531
Jore, K. P., Broeils, A. H., & Haynes, M. P. 1996, AJ, 112, 438
Kamphuis, J., Sijbring, D., & van Albada, T. S. 1996, A&AS, 116, 15
Karachentsev, I. D. 1980, ApJS, 44, 137
Knapp, G. R., Kerr, F. J., & Henderson, A. P. 1979, ApJ, 234, 448
Knapp, G. R., Kerr, F. J., & Williams, B. A. 1978, ApJ, 222, 800
Kraan-Korteweg, R. C., van Driel, W., Briggs, F., Binggeli, B., & Mostefaoui, T. I. 1999, A&AS, 135, 255
Krumm, N., & Salpeter, E. E. 1980, AJ, 85, 1312
Lake, G., & Schommer, R. A. 1984, ApJ, 280, 107
Lewis, B. M. 1985, ApJ, 292, 451
Lewis, B. M. 1987, ApJS, 63, 515
Lewis, B. M., & Davies, R. D. 1973, MNRAS, 165, 213
Lewis, B. M., Helou, G., & Salpeter, E. E. 1985, ApJS, 59, 161
Lo, K. Y., & Sargent, W. L. 1979, ApJ, 227, 756
Magri, C. 1994, AJ, 108, 896
Mahdavi, A., Boehringer, H., Geller, M., & Ramella, M. 1997, ApJ, 483, 68
Mamon, G. A. 1986, ApJ, 307, 426
Marcum, P. 1994, Star Formation Structure and Evolution of Galaxies in Loose Groups: the Environmental Connection, Ph.D. Thesis (University of Wisconsin, Madison)
Martin, M. C. 1998, A&AS, 131, 73
Matthews, L. D., van Driel, W., & Gallagher, J. S. 1998, AJ, 116, 1196
Matthews, L. D., & van Driel, W., 2000, A&AS, 143, 421
Matthews, L. D., van Driel, W., & Monnier-Ragaigne, D. 2001, A&AS, 365, 1
Mihos, J. C., Walker, I. R., Hernquist, L., Mendes de Olivera, C., & Bolte, M. 1995, ApJ, 447, L87
Mirabel, I. F. 1982, ApJ, 260, 75
Mirabel, I. F., & Sanders, D. B. 1988, ApJ, 335, 104
Mirabel, I. F., & Wilson, A. S. 1984, ApJ, 277, 92
Mould, J. R., Akeson, R. L., Bothun, G. D., et al. 1993, ApJ, 409, 14
Mulchaey, J. S., & Zabludoff, A. J. 1998, ApJ, 496, 73
Mulchaey, J., Davis, D., Mushotzky, R., & Burstein, D. 1996, ApJ, 456, 80
Mundell, C. G., Pedlar, A., Axon, D. J., Meaburn, J., & Unger, S. W., 1995, MNRAS, 277, 641
Nolthenius, R. A. 1993, ApJS, 85, 1
Nordgren, T. E., Chengalur, J. N., Salpeter, E. E., & Terzian, Y. 1997, AJ, 114, 913
Oosterloo, T., & Shostak, S. 1993, A&AS, 99, 379
Ostriker, J. P., Lubin, L. M., & Hernquist, L. 1995, ApJ, 444, L61
Paturel, G. 1998, private communication
Peterson, C. J., Rubin, V. C., Ford Jr., W. K., & Thonnard, N. 1978, ApJ, 219, 31
Peterson, S. D. 1979, ApJS, 40, 527
Peterson, S. D., & Shostak, G. S. 1974, AJ, 79, 767
Rhee, M.-H., & van Albada, T. S. 1996, A&AS, 115, 407
Richter, O.-G., & Huchtmeier, W. K. 1991, A&AS, 87, 425
Richter, O.-G., & Sancisi, R. 1994, A&A, 290, L9
Rood, H. J, & Dickel, J. R. 1976, ApJ, 205, 346
Rose, J. A. 1977, ApJ, 211, 311
Rose, J. A. 1979, ApJ, 231, 10
Sancisi, R., Allen, R. J., & Sullivan III, W. T. 1979, A&A, 78, 217
Sanduleak, N., & Pesch, P. 1987, ApJS, 63, 809
Schneider, S. E., Helou, G., Salpeter, E. E., & Terzian, Y. 1986a, AJ, 92, 742
Schneider, S. E., Salpeter, E. E., & Terzian, Y. 1986b, AJ, 91, 13
Schneider, S. E., Thuan, T. X., Magri, C., & Wadiak, J. E. 1990, ApJS, 72, 245
Scodeggio, M., & Gavazzi, G. 1993, ApJ, 409, 110
Shostak, G. S. 1975, ApJ, 198, 527
Shostak, G. S. 1978, A&A, 68, 321
Silverglate, P. R., & Krumm, N. 1978, ApJ, 224, L98
Staveley-Smith, L., & Davies, R. D. 1987, MNRAS, 224, 953
Staveley-Smith, L., & Davies, R. D. 1988, MNRAS, 231, 833
Sulentic, J. W., & Arp, H. 1983, AJ, 88, 489
Theureau, G., Bottinelli, L., Coudreau-Durand, N., et al. 1998, A&AS, 130, 333
Thonnard, N., Rubin, V. C., Ford Jr., W. K., & Roberts, M. S. 1978, AJ, 83, 1564
Thuan, T. X., & Martin, G. E. 1981, ApJ, 247, 823
Tifft, W. G., & Cocke, W. J. 1988, ApJS, 67, 1
van der Burg, G. 1985, A&AS, 62, 147
van Driel, W., & van Woerden, H. 1991, A&A, 243, 71
van Moorsel, G. A. 1983, A&AS, 53, 271
Wardle, M., & Knapp, G. R. 1985, AJ, 91, 23
Wevers, B. M. H. R., van der Kruit, P. C., & Allen, R. J. 1986, A&AS, 66, 505
Williams, B. A. 1985, ApJS, 290, 462
Williams, B. A., & Rood, H. J. 1987, ApJS, 63, 265
Williams, B. A., McMahon, P. M., & van Gorkom, J. H. 1991, AJ, 101, 1957
Xue, Y.-J., & Wu, X.-P. 2000, ApJ, 538, 65
Yun, M. S., Ho, P. T. P., & Lo, K. Y. 1994, Nature, 372, 530
Zwaan, M. A. 2000, Atomic Hydrogen in the Local Universe, Ph.D. Thesis, University of Groningen
Zwaan, M. A. 2001, MNRAS, 325, 1142